UNIVERSITY OF GAZİANTEP

GRADUATE SCHOOL OF

NATURAL & APPLIED SCIENCES

RELATIVE INTENSITY NOISE OF MODE-LOCKED LASERS UTILIZING SINUSOIDALLY CHIRPED FIBER BRAGG GRATING

M. Sc. THESIS

IN

ELECTRICAL-ELECTRONICS ENGINEERING

BY

ERHAN ERSOY

JUNE 2013

Relative Intensity Noise of Mode-Locked Lasers

Utilizing Sinusoidally Chirped

Fiber Bragg Grating

M.Sc. Thesis

in

Electrical-Electronics Engineering

University of Gaziantep

Supervisor

Assoc. Prof. Dr. Nuran DOĞRU

by

Erhan ERSOY

June 2013

Name of the thesis: Relative intensity noise of mode-locked laser utilizing sinusoidally chirped fiber Bragg grating.

Name of the student: Erhan ERSOY
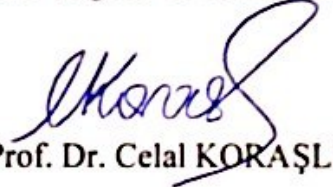
Exam date: 10.06.2013

Approval of the Graduate School of Natural and Applied Sciences
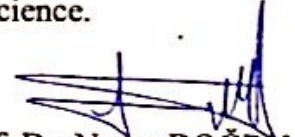
Assoc. Prof. Dr. Metin BEDİR

Director

I certify that this thesis satisfies all the requirements as a thesis for the degree of Master of Science.

Prof. Dr. Celal KORAŞLI

Head of Department

This is to certify that we have read this thesis and that in our consensus/majority opinion it is fully adequate, in scope and quality, as a thesis for the degree of Master of Science.

Assoc. Prof. Dr. Nuran DOĞRU

Supervisor

Examining Committee Members (Title and Name-surname)

Prof. Dr. Beşire GÖNÜL (Chairman)

Prof. Dr. Arif NACAROĞLU

Assoc. Prof. Dr. Nuran DOĞRU

I hereby declare that all information in this document has been obtained and presented in accordance with academic rules and ethical conduct. I also declare that, as required by these rules and conduct, I have fully cited and referenced all material and results that are not original to this work.

Erhan ERSOY

ABSTRACT

RELATIVE INTENSITY NOISE OF MODE-LOCKED LASERS UTILIZING SINUSOIDALLY CHIRPED FIBER BRAGG GRATING

ERSOY, Erhan

M.Sc. in Electrical-Electronics Eng.

Supervisor: Assoc. Prof. Dr. Nuran DOĞRU

June 2013, 78 pages

The relative intensity noise (RIN) of a mode-locked hybrid soliton pulse source (HSPS) utilizing a sinusoidally chirped fiber Bragg grating (FBG) is investigated using the time-domain solution of coupled wave equations and rate equations which include both spontaneous and carrier density noise. The effect of some laser diode and grating parameters on the RIN of the HSPS are also described. The numerical results show that most of the parameters affect the system operation even without noise. However, noise increases with increasing linewidth enhancement factor, gain saturation parameter, spontaneous coupling factor and field coupling factor. Noise is also extremely sensitive to the RF and DC currents. RIN reduction at the fundamental frequency (2.5 GHz) is possible in a mode-locked HSPS utilizing a sinusoidally chirped Gaussian apodized FBG when compared with a HSPS with linearly chirped gratings. 9.64 dB noise reductions are obtained when the standard parameters are used. Furthermore, it is also shown that a HSPS utilizing a sinusoidally chirped FBG produces shorter pulses than linearly chirped FBG with and without noise.

ÖZET

FİBER BRAGG IZGARA KULLANAN MOD-KİLİTLİ LASERİN BAĞIL ŞİDDET GÜRÜLTÜSÜ

ERSOY, Erhan

Yüksek Lisans Tezi, Elektrik-Elektronik Müh. Bölümü

Tez Yöneticisi: Doç. Dr. Nuran DOĞRU

Haziran 2013, 78 sayfa

Sinüslü chirped fiber Bragg ızgara (FBG) kullanan mod-kilitli karışık soliton darbe kaynağının (HSPS) bağıl şiddet gürültüsü (RIN) spontane ve taşıyıcı gürültüyüde içeren çift dalga (coupled wave equations) ve oransal denklemlerinin (rate equations) zaman domaninde çözümü kullanılarak tanımlandı. Ayrıca bazı lazer diyot ve ızgara parametrelerinin karışık soliton darbe kaynağının (HSPS) bağıl şiddet gürültüsü üzerindeki (RIN) etkileride tanımlandı. Sayısal sonuçlar, gürültünün olmadığı durumda bile bir çok parametrenin sistemin çalışmasını etkilediğini gösteriyor. Bununla birlikte gürültü çizgi genişliği (linewidth enhancement) artma faktörü, kazanç doyma (gain saturation) faktörü, spontane kavrama (spontaneous coupling) faktörü ve alan kavrama (field coupling) faktörünün artması ile artmıştır. Gürültü aynı zamanda RF ve DC akımlarına da aşırı derecede duyarlıdır. Sinüslü chirped fiber Bragg ızgara (FBG) kullanan mod-kilitli karışık soliton darbe kaynağı (HSPS), doğrusal azalan mod-kilitli HSPS ile karşılaştırıldığı zaman, temel frekansta (2.5 GHz) RIN azaltılmasının mümkün olduğu bulundu. Standart parametreler kullanıldığı zaman gürültüde 9.64 dB'lik bir zayıflama elde edilmiştir. Ayrıca, sinüslü chirped fiber Bragg ızgara kullanan karışık soliton darbe kaynağının (HSPS) gürültülü ve gürültüsüz durumda doğrusal chirped fiber Bragg ızgaradan daha kısa darbler ürettiği gösterilmiştir.

Anahtar Kelimeler: Bağıl şiddet gürültüsü, taşıyıcı gürültü, aktif mod kilitleme, fiber Bragg ızgara, karışık soliton darbe kaynağı, yarıiletken lazerler, sinüslü chirped, ultra kısa darbe üretimi.

''To my family''

ACKNOWLEDGEMENTS

TABLE OF CONTENTS

LIST OF FIGURES

LIST OF TABLES

LIST OF SYMBOLS / ABBREVIATIONS

AR	Anti-Reflection Coating
HR	High Reflectivity Coating
α	Loss
α_{int}	Total Internal Loss
α_c	Cladding Loss
α_h	Linewidth Enhancement Factor
B	Bimolecular Recombination Factor
β	Propagation Constant
β_o	Bragg Propagation Constant
β_{sp}	Spontaneous Emission Parameter
C	Chirped Parameter
dt	Time Step Size
dz	Distance Step Size
δ	Deviation from real part of propagation constant (β-β_o)
δn	Amplitude of Refractive Index Perturbation
Δn	Carrier Induced Refractive Index Change
Δz	Length of Section
E	Electric Field
ε	Gain Saturation Parameter
f_m	Mode Locking Frequency
F	Forward Propagation Field
F_N	Carrier Noise
FBG	Fiber Bragg Grating

HSPS	Hybrid Soliton Pulse Source
Φ	Chirped Function
g	Gain
γ	(Defined)
η	Field Coupling Factor between Laser and Fiber
I_{rf}	Amplitude of RF Current
I_{dc}	DC Bias Current
I_{th}	Threshold Current
j	Complex Number
κ	Coupling Factor
κ_p	Peak of Gaussian κ variation
L_l	Length of Laser
L	Length of Grating[*]
L_c	Length of External Cavity
L_H	Half-Width of the Apodization Function Profile
LED	Light Emitting Diode
λ	Operating Wavelength
λ_o	Bragg Wavelength
Λ	Pitch of the Grating
m	Modulation Index
M	Number of Grating sections
M_B	Order of Bragg Grating
n	Refractive Index
n_{eff}	Effective Refractive Index (Modal Index)
n_{co}	Refractive Index of Unmodified Fiber Core
n_l	Refractive Index of Laser Cavity (Active Region)
N	Electron Density

N_o	Transparency Carrier Density
π	Pi Constant (3,14…..)
ρ	Reflectivity (Field)
ρ_p	Desired Peak Reflectivity (Field)
r_1	Field Reflectivity of Left Facet (HR Coating)
r_2	Field Reflectivity of Right Facet (End of Grating)
r_3	Field Reflectivity of AR Coating
R	Reverse Propagating Field
R_{sp}	Spontaneous Emission Rate
s	Spontaneous Emission into the Fields
s_f	Spontaneous Emission Noise into the Forward Wave
s_r	Spontaneous Emission Noise into the Reverse Wave
t	Time
σ	DC Coupling Coefficient
$\hat{\sigma}$	DC "self-coupling" Coefficient
τ_n	Carrier Lifetime
Γ	Confinement Factor
z	Space Variable in Cartesian Coordinates
RIN	Relative Intensity Noise
TBP	Time-Bandwidth Product
Ψ	Wave Function
OTDM	Optical Time Division Multiplexing
DWDM	Dense Wavelength Division Multiplexing

CHAPTER 1

INTRODUCTION

The semiconductor laser, first discovered in 1962, [1-2] was thought to be breakthrough invention that would revolutionize industry. As early as the late 1960s and early 1970s there were patents and articles proclaiming the utility of technology for optical data storage and fiber optic and free space communications [3]. The dynamic behavior of semiconductor laser due to optical feedback has been the subject of considerable experimental and theoretical interest [4-5]. However, the noise characteristics of semiconductor laser are among the fundamental properties of the laser because noise limits the performance in communications and high-speed optical sampling [6-7]. Operating characteristic of a semiconductor laser is strongly affected by external optical feedback [8] as it was observed long ago. Theoretical investigations of optical feedback effects are usually based on the Lang and Kabayashi (LK) rate equations [4] which have been shown to contain all the dominant effect observed experimentally for low to moderate coherent optical feedback levels. The relative intensity noise (RIN) properties of semiconductor laser subject to optical feedback have been investigation theoretically by Petermann [9] using the LK model.

Diode laser are very sensitive to optical feedback due to the low Q-factor and high gain of laser cavity. The optical feedback techniques lead to many attractive properties of diode laser such as [10];

1. Linewidth reduction

2. Tunability

3. Improved spatial and tempered coherence

4. Mode-Locking

The relative intensity noise (RIN) has been studied in detail with respect to the change of external cavity length and the reflectivity of the external cavity. It was investigated for different feedback levels [11-12] by using Langevin noise source for external cavity laser.

The numerous phenomena associated with external optical feedback are conventionally grouped into five distinctive regimes, defined in terms of the external cavity length and optical strength [10].

1. Stable regime where linewidth is narrowed or broadened depending on the phase of the optical feedback.

2. Conditionally stable.

3. Stable single mode operation is obtained with linewidth reduction.

4. Unstable operation with coherence collapse.

5. Stable operation with significant linewidth reduction.

The RIN remains essentially constant as the optical feedback is increased until coherence collapsed is induced, whereupon there is a dramatic increase in the RIN. The RIN remains very high as the optical feedback is increased, until stable external cavity laser operation is obtained in regime five, which is signified by drop in the RIN. These results showed that higher optical feedback levels were required to enter regime four and five as the bias current was increased [13].

This led to increase in research on strong feedback external cavity laser for optical communication system. There are several strong feedback external cavity lasers frequency selective schemes which have been reported in literature. Some of them are;

1. Feedback from a grating [14]

2. Feedback from high Q-narrow band resonator [15]

3. Feedback from a Fiber Bragg Grating (FBG) reflection [16]

In this thesis, FBG is used as an external cavity in strong external cavity laser. The strong feedback can only be obtained with an anti-reflection (AR) coating of one laser facet as in our model.

Some period, most of the researchers concentrate only on the weak feedback conditions. The detailed first study of noise and modulation performance under strong external feedback conditions were written by Ferreira *et al* [17].

Short pulse generation from semiconductor laser is currently very active research area. There are several ways to obtain short pulses from semiconductor laser. One of them is mode-locking technique. The word mode-locking describes the locking of multiple axial modes in a laser cavity. The history of mode-locking is a progression of new and better ways to generate shorter and shorter pulses, and of improvements in the understanding of mode-locking process. The first indication of mode-locking appears in the work of Gürs and Müller [18-19] on ruby lasers, and Statz and Tang [20] on He-Ne lasers. The pioneering studies clearly identifying the mechanism were written in 1964 by DiDomenico [21], Hargrove *et al*. [22], and Yariv [23]. Hargrove *et al*. who achieved mode-locking by internal loss modulation inside resonator. This is the case of active mode-locking. Shorter pulses with less timing jitter can be obtained by active mode-locking the laser [24]. Active mode-locking is accomplished by applying a current waveform to gain section, including a DC bias close to the threshold value plus an RF component that can be varied in amplitude and frequency at a frequency equal to inverse round trip period. Hybrid soliton pulse source (HSPS) is one such device, developed as a pulse source for soliton transmission system [25]. HSPS was first experimentally shown to operate quite well as soliton pulse source in 1993, by Morton *et al*. at AT&T Labs. However, the theoretical model of the mode-locked HSPS has been developed by Sayın in 1999 [28]. HSPS consists of a multi- quantum well (MQW) laser, a certain length of fiber and a FBG. Using linearly chirped FBG in the HSPS results in a tunable system over the range of mode-locked frequencies, as the cavity length is wavelength dependent [25]. Because of this property and its very high power, HSPS become very attractive pulse source for high-speed soliton transmission systems. The major parameters of a pulse source are its pulsewidth, pulse shape, operating wavelength, time bandwidth product (TBP) and repetition rate of the source must be exactly the same as the clock rate in transmission system. Standard mode-locked laser have a fixed cavity length.

This determines the operating frequency which is close to the cavity resonance frequency. The required pulsewidth depends on the operating bit rates of the transmission system. Shorter pulsewidth requires higher average power levels for soliton propagation, while longer pulses tend to interact with neighboring pulses. Pulsewidths are typically chosen to occupy approximately 1/5 of the operating bit period, giving a range 20 ps to 80 ps for systems operating from 10 Gbit/s to 2.5 Gbit/s. The optimum pulse shape for a standard soliton transmission system would be sech^2 in shape, to match the soliton shape. However, it has been shown that symmetrical pulse shape such as Gaussian shaped will also acceptable and work [8].

One major restriction on the pulse source is that the output waveform must be tramsform limited, or close to transform limited, to allow optimum system operation. In order to be transform limited pulse, the TBP of the pulse must lie in the range of 0.3-0.5 [26], which is TBP of sech^2 and Gaussian pulses, respectively. This restriction is reduced somewhat in systems employing sliding-frequency guiding filters, which are more tolerant to lower fidelity pulse waveforms. The realization of long distance soliton based transmission systems requires a reliable stable source of transform limited pulses of the correct pulsewidth and at the wavelength peak of erbium-doped fiber amplifier chain (1.55μm). A practical system may operate at 2.488 GHz with pulsewidth of around 50 ps. The HSPS has been theoretically demostrated in the mode-locking regime at 2.5 GHz [28]. A model for the mode-locked HSPS has already been reported by Ozyazıcı *et. al.* [27] and more completed scheme including the grating parameters and the laser diode drive conditions on the response of the HSPS has been investigated in [28]. Although many theoretical models for modulation response and mode locking performance of strong feedback external cavity lasers have been described in the literature [29-30], until a few years, no studies have been made showing noise characterstics of these lasers at the mode locked condition. A few years ago, how the spontaneous and carrier noise affects the output pulse of mode locked HSPS utilizing linearly chirped FBGs such as uniform,Gaussian apodized, linearly chirped uniform and linearly chirped Gaussian apodized and RIN spectrum of HSPS and most effective noise parameters were investigated by Dogru in [8]. A new kind of grating profile with sinusoidally chirped grating periods was introduced by Zhang et al. for DWDM applications [31-33]. Such a structure produces nearly ideal reflection spectra, giving a wider bandwidth,

steep edges, and large bandwidth utilization [31-33] Dogru theoretically designed a sinusoidally chirped FBG for mode-locked applications [34]. The results showed that the sinusoidally chirped grating produced shorter pulses than the linearly chirped grating. It also increased mode-locking over a much larger center frequency range (2.1–3.2 GHz), when compared with the range of a linearly chirped Gaussian apodized FBG (2.1–2.95 GHz) [35]. But, there is no study showing the RIN characteristics of HSPS utilizing nonlinear chirp (sinusoidally) FBG.

In this thesis, RIN of mode-locked HSPS utilizing sinusoidally chirped Gaussian apodized FBG is investigated for different values of laser parameters and RF and DC currents when both spontaneous and carrier noise are taken into account. Results are provided with linearly chirped Gaussian apodized FBG.

In Chapter 2, mode-locking semiconductor laser, active mode-locking technique and structure of the HSPS are explained.

Results of the mode-locked HSPS with spontaneous noise, carrier noise and RIN are given in Chapter 3. Spontaneous, carrier and relative intensity noise (RIN) are also explained in this chapter.

RIN spectrum of mode-locked HSPS with FBG is indicated in Chapter 4. Effect of the RF and DC current, anti-reflection coefficient, reflectivity, external cavity length and important noise parameters of laser on RIN are also determined in this chapter. In addition, RIN reduction using sinusoidally chirped Gaussian-apodized FBG is also presented in Chapter 4.

 In Chapter 5, results obtained from the mode-locked HSPS without and with noise using sinusoidally chirped Gaussian-apodized FBG is concluded.

CHAPTER 2

MODELING OF HYBRID SOLITON PULSE SOURCE (HSPS)

2.1 Introduction

Laser diodes are electrically pumped semiconductor lasers in which the gain is generated by an electrical current flowing through a p–n junction or a p–i–n structure. In such a heterostructure, electrons and holes can recombine, releasing the energy portions as photons. This process can be spontaneous, but can also be stimulated by incident photons, in effect leading to optical amplification, and with optical feedback in a laser resonator to laser oscillation [37-46]. Without pumping, most of the electrons are in the valence band. A pump beam with photon energy slightly above the bandgap energy can excite electrons into a higher state in the conduction band, from where they quickly decay to states near the bottom of the conduction band. At the same time, the holes generated in the valence band move to the top of the valence band. Electrons in the conduction band can then recombine with these holes, emitting photons with energy near the bandgap energy. This process can also be stimulated by incoming photons with suitable energy. Most semiconductor lasers are laser diodes, which are pumped with an electrical current in a region where an n-doped and a p-doped semiconductor material meet. However, there are also optically pumped semiconductor lasers, where carriers are generated by absorbed pump light. Common materials for semiconductor lasers are GaAs, AlGaAs, GaP, GaN, InGaAs, InP and GaInP [37-46].

Although there is a great variety of a different semiconductor laser, spanning wide parameter regions and many different application areas, the basic principle of operation is the same for each type of laser. For the laser action, there are three processes.

These three processes are;

1) Photon absorption
2) Stimulated emission
3) Spontaneous emission.

As we all know that atoms and molecules can exist only in certain energy states. The state of lowest energy is called the ground state (E_1); all other states have more energy than the ground state and are called excited states (E_2). Each excited state, of which there are many, has a fixed amount of energy ($hv_{12}=E_1-E_2$) over and above that of the ground state. Under ordinary conditions, almost all atoms and molecules are in their ground states. Three types of processes are possible for a two-level atomic system as shown in the Fig. 2.1. In the first, an incoming photon excites the atomic system from a lower energy state into a higher energy state. This is called absorption or sometimes ***stimulated absorption*** as shown in Fig. 2.1a. It is called stimulated absorption because of the fact that the atoms absorb the incident energy at certain frequencies only. Stimulated absorption occurs when a photon strikes an atom with just exactly the proper energy to induce an electronic transition between two energy states. The absorption depends on the population difference and the refractive index of the medium[47].

Under the influence of a quantum, an electron may be transferred from the conduction band to hole on the valance band. Such a transfer will be accompanied by the emission of a light quantum identical in frequency, direction of propagation and polarization to the quantum which produced the emission. This process is connected with an increase of the field energy and is called ***stimulated emission*** as shown in Fig. 2.1c. In case of stimulated emission, atoms in an upper energy level can be triggered or stimulated in phase by an incoming photon of a specific energy. The incident photon must have an energy corresponding to the energy difference between the upper and lower states. The emitted photons have the same energy as incident photon. These photons are in phase with the triggering photon and also travel in its direction. Besides stimulated absorption and stimulated emisson, a third process of spontaneous emission may take place. If an atom is in an excited state, it may spontaneously decay into a lower energy level after some time, releasing energy in the form of a photon, which is emitted in a random direction. This process is called

spontaneous emission as shown in Fig 2.1b[8]. Spontaneous emission is completely isotropic. Stimulated processes, on the other hand, have a built-in preference for emission in the direction of the incident flux of photons.
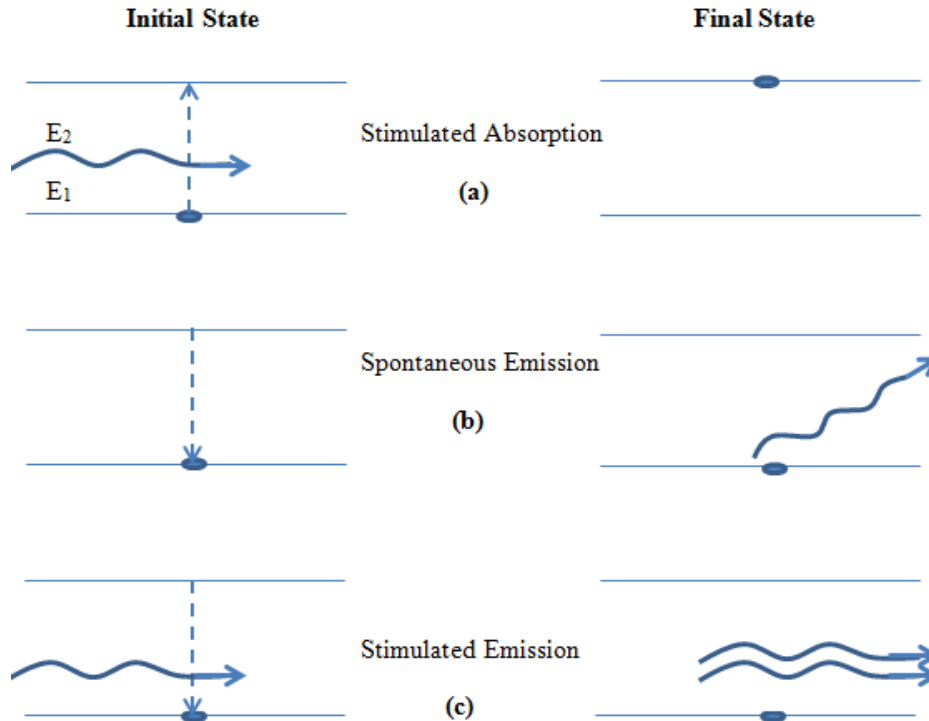
Figure 2.1 Energy level diagram illustrating (a) absorption, (b) spontaneous emission and (c) stimulated emission. The black dot indictes the state of the atom before and after the transition [8].

In simple cases, a laser transition, on which optical gain occurs as a result of stimulated emission, involves only two (non-degenerate) energy levels of the active atoms or ions of the gain medium: an upper and a lower laser level. The transition cross section for absorption and for stimulated emission must then be the same and a positive net gain can occur only when the population of the upper laser level is higher than that of the lower level. In other words, more laser-active ions are in the upper state than in the lower state. This condition of the laser medium is called *population inversion*. Population inversion is a state of the system which deviates from thermal equilibrium: in thermal equilibrium, the population of the lower level is always higher, and a positive net gain can never occur. Formally, population inversion is sometimes described as a state with a negative temperature. In many cases, it is achieved by optical pumping.

The light output and diode drive current characteristic of an ideal semiconductor laser are given in Fig. 2.2. At low diode currents only spontaneous radiation is emitted. Output power from a diode laser increases linearly with the drive current excess above the threshold current as seen in Fig. 2.2. This steeply rising light output curve is extrapolated backward to the zero light output intercept to define the threshold current (I_{th}); the weak incoherent light emission for currents below threshold is due to the spontaneous recombination of carrier such as occurs in LEDs [48] as shown in Figure 2.2 region (a). Region (b) is non-linear transition region, where the spontaneous and stimulated emission regimes are both significant and the brightness of device increases rapidly. Such a device is called a superradiant LED. The stimulated emission region, characterized by a steep slope of light output/current is shown in region (c).
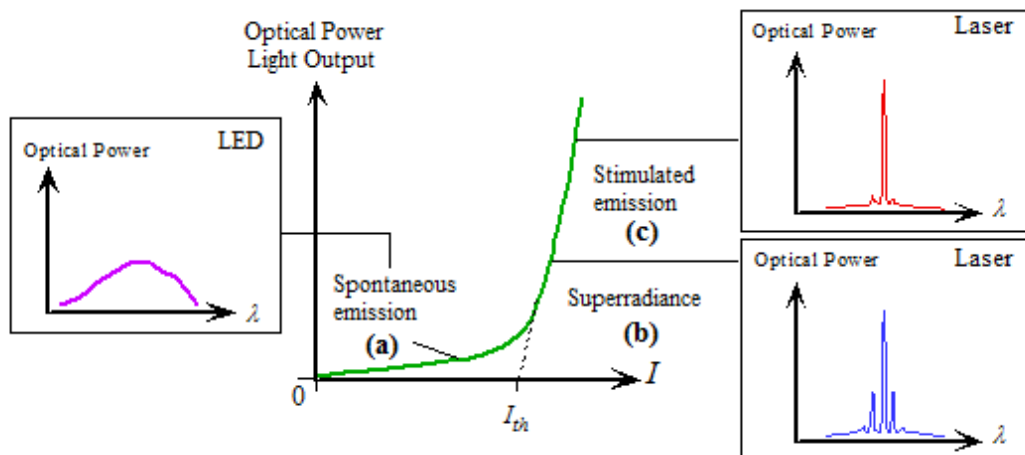
Figure 2.2   Light output (Optical Power) - Current characteristic of an ideal semiconductor laser and corresponding output spectrum of a laser diode. [4]

2.2   Mode Locked Lasers

Laser beam properties such as direction and divergence of the beam, the beam profile, and the wavelength and frequency characteristics of the laser within the wavelength region of the laser gain bandwidth are determined largely by the laser mirrors. The factors determining those properties include mirror curvature, surface quality, and reflectivity as well as separation and location, assuming that the

structure holding the mirrors are a secure, vibration-free structure. The unique electromagnetic wave properties produced by the mirrors are referred to as modes.

When the beam is developing within the mirror cavity, traveling back and forth, certain wavelengths within the gain bandwidth of the laser tend to be more enhanced than others. These are wavelengths (or frequencies) in which the light beam in the cavity forms a *standing wave* [49]. Such an effect occurs when an exact number of half-wavelengths of the light fit within the separation distance between the mirrors. Typically there will be several hundred thousand wave peaks for each standing wave that occurs within the cavity. Hence, each standing wave must have a wavelength such that an integral number of oscillating waves fits in the space separating the mirrors. If more than one standing wave is present, each standing wave (*longitudinal mode*) will be separated in frequency from the next one by a fixed exact amount that depends upon the laser cavity length L_l [49].

Stationary waves of frequency

$$ f = \frac{nc_o}{2L_l n_l} \tag{2.1} $$

where c_o is the velocity of light in vacuum (cm/sec), L_l is the laser diode length (cm), n_l is the active region refractive index, and n is the any integer which are the directed along the laser axis are called *longitudinal (axial) modes* of the laser. Each discrete standing wave is referred to as a longitudinal mode associated with the laser cavity [8].

The presence of more than one longitudinal mode involves many light beams traveling exactly the same path through the amplifier but differing in wavelength depending upon the total number of wave cycles that fit between the mirrors are called *transverse modes*. Contrary to this, different transverse modes involve slightly different optical paths through the amplifier and thus have slightly different directions when they emerge from the laser. Because of the different optical path lengths, they also have slightly different frequencies. Each of these stable modes evolves because the light traveling that particular pathway recurs exactly from one round trip of the beam to the next, therefore developing into a steady beam. Each transverse mode traveling over its unique path might also consist of several

longitudinal modes separated in frequency according to Equation (2.1) [49]. Electric field configurations which exist in laser cavities are of the tansverse electromagnetic type, represented as TEM_{qmn} where q is the longitudinal mode order number and m, n are the transverse mode order numbers. The lowest-order transverse mode, known as the TEM_{00} mode, travels down the central axis of the laser gain medium [49].

Mode-locked semiconductor laser diodes offer the possibility of producing small, and reliable sources of stable picosecond pulses over a wide wavelength ranges and with moderate peak powers. They can be used in telecominication system for time-division multiplexing or for high-bit rate system using an external modulator. Semiconductor laser are ideal candidtes for use in practical commerical electrooptic sampling systems due to their small size, low cost, low noise and small timing jitter in comparision to the use of the more complex and less reliable sources as pulse – compressed YAG lasers.

It is possible in a laser that a very wide gain bandwidth to obtain thousands of longitudional modes operates simultaneously. If these modes are all locked in phase so that they all oscillate upward or downward together, they will combine in a way that produces chain of very short pulses separated in time by Δt_{sep} and the process of fixing the frequency seperation and phase differences of the excited modes can be defined as *"mode-locking"*. [49]

Mode-locking operation can be classified into two regimes, active and passive mode-locking. In both of these methods, there is a gain/loss modulation mechanism. In active mode-locking, a fast acuosta-optic device operating at a frequency close to the repetiton rate of the cavity initiates the generation of the ultra short pulses. In passive mode-locking, an intensity-dependent property as the gain/loss switching mechanism. In this case high intensity fluctuations experience higher order optical gain inside the resonator. This behavior forces the modes to oscillate in phase to generate high-intensity pulses. A third type of mode-locking called "self-locking", is also possible. In self-locking, ultra short pulses can be obtained spontaneously without employing an external modulator or other mode-locking element. However, due to unstable and uncontrollable nature of self-locking, this method is very rarely used.

Short pulse generation from mode-locked semiconductor lasers is currently a very active research area. Because picosecond optical pulse are required for many applications including micromachining, medical imaging, optical communications, higher order harmonic generation, and measuring of fundamental constants of nature. The technique of mode-locked can be used to generate such pulses from lasers with pulse emission occuring at the round-trip frequency of the laser cavity. Mode-locking of external cavity lasers is a well-established technique, with picosecond and subpicosecond pulses being achieved. Mode-locked HSPS is a kind of external cavity lasers where FBG is used as external cavity. Structure of this laser is explained in section 2.3.

2.3   Structure of the HSPS

The hybrid soliton pulse source (HSPS) indicated in Figure 2.3 is demonstrated first by Morton et al. [25]. HSPS is modeled by using couple-mode equations. HSPS is a strong external feedback device providing stable and single mode operation and it consists of mainly three sections as shown in Figure 2.3.
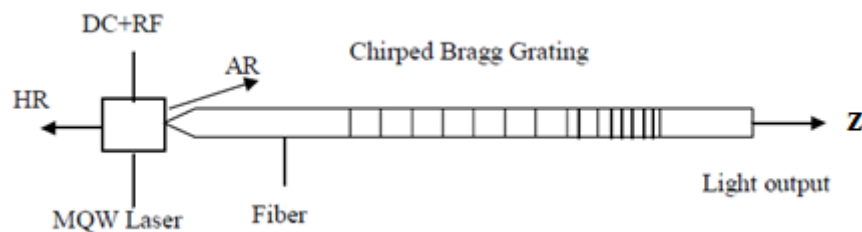
Figure 2.3 Schematic of Hybrid Soliton Pulse Source (HSPS) with chirped FBG.

The HSPS system is made up of a multiple-quantum-well (MQW) semiconductor laser, a lensed fiber and fiber Bragg grating (FBG). One facet of the diode is high reflectivity (HR) coated and the other anti-reflection (AR) coated. The output power is taken through the grating.

The effective refractive index variation of the Bragg grating along the propogation direction (z) is given as,

$$n(z) = n_{co} + \Delta n(z)[1 + m\cos(\frac{2\pi}{\Lambda(z)} z)] \qquad (2.2)$$

where n_{co} is the unperturbed effective index of the fiber, $\Delta n(z)$ represents the dc index change , spatially averaged over a grating period, and m is the modulation index of the grating. The z-dependent grating period $\Lambda(z)$ is sinusoidally chirped.

$$\Lambda(z) = \Lambda_o + \frac{\Lambda_o^2}{2\pi} C\sin(\frac{2\pi p}{L} z) \qquad (2.3)$$

where $\Lambda_o = \lambda_o / 2n_{co}$ is the pitch of the unchirped Bragg grating at the operating wavelength λ_o . C is the chirp indicates the number of periods of the sine function over the fiber grating where 0.5< p < 1 and z is *(-L/2, L/2)*. The chirp is limited to a single sinusoidal period.

The time-domain propagation equations for the forward and backward propogating electric field components, F(z,t) and R(z,t), are written as,

$$\frac{dF}{dz} = -j\left(\delta + \frac{2\kappa(z)}{m} - \frac{1}{2}\frac{d\varphi}{dz}\right)F - j\kappa(z)R + s_f \qquad (2.4)$$

$$\frac{dR}{dz} = j\left(\delta + \frac{2\kappa(z)}{m} - \frac{1}{2}\frac{d\varphi}{dz}\right)R + j\kappa(z)F + s_r \qquad (2.5)$$

where $\kappa(z)$ is the coupling coefficient between the forward and reverse waves, δ is the deviation of the propogation constant β from the Bragg condition ($\delta=\beta-\beta_o=\beta-\pi/\Lambda_o$), and φ is the grating chirp,

where

$$\varphi = -C\sin\left(\frac{2\pi p}{L} z\right)z \qquad (2.6)$$

13

The loss in the fiber and grating can be neglected because the fiber is only a few centimeters long. The parts inside the parentheses in (2.4) and (2.5) are designated as the dc "self-coupling" coefficient [34, 50-52].

The spontaneous noise coupled into the forward and reverse fields is represented as s_f and s_r, respectively. The spontaneous emission fields coupled to the forward and reverse fields have equal amplitudes [34, 50-52], it means that $s(z,t) = s_f(z,t) = s_r(z,t)$. This emission is assumed to have a Gaussian distribution and to satisfy the correlation constraints:

$$< s(z,t)s^*(\dot{z},t) >= \beta_{sp}R_{sp}\delta(t-\dot{t})\delta(z-\dot{z})/v_g$$

and

$$< s(z,t)s^*(\dot{z},t) >= 0 \qquad\qquad (2.7)$$

where $R_{sp} = BN^2/L_l$ is the electron-hole recombination rate per unit length contributing to the spontaneous emission. Here, B is the radiative recombination coefficient, L_l is the length of the lasing section, N is the carrier density, β_{sp} is the spontaneous coupling factor, and v_g is the group velocity of the light in the cavity.

Results of mode-locked HSPS with noise are given in next chapter. In this chapter, spontaneous noise, carrier noise and RIN are explained. Then mode-locked pulses are analyzed for sinusoidally chirped Gaussian apodized FBG with both spontaneous noise and carrier noise.

CHAPTER 3

SPONTANEOUS AND CARRIER NOISE IN MODE-LOCKED HSPS

3.1   Introduction

In this chapter, types of noise in the laser will be described. Then the output of HSPS will be investigated for sinusoidally chirped fiber Bragg gratings (FBGs) when both spontaneous and carrier noise are taken into account. In order to find out whether HSPS is properly mode-locked or not, their TBP (time bandwitdh product) will be investigated at the mode-locking frequency of 2.5 GHz. The frequency range of HSPS mode-locked will also be identified. We do all these calculations to show how the noise affects the operation of mode-locked hybrid soliton pulse source (HSPS).

The peak reflectivity of fiber grating is taken as 0.5. Other standard parameters for the mode-locked HSPS program are given in Table 3.1.

Table 3 1 Standard parameters for the Hybrid Soliton Pulse Source (HSPS) mode-locking program [8].

Parameter	Symbol	Standard Value	Unit
Differential Gain	a_0	10×10^{-16}	cm^2
Gain Saturation Parameter	ε	2×10^{-17}	cm^3
Spontaneous Emission Parameter	β_{sp}	5×10^{-5}	
Field Coupling Factor	η	0.8	-
Field Reflectivity of AR Coating	r_3	0.01	-
Field Reflectivity of Left Facet	r_1	0.9	-
Field Reflectivity of Left Facet	r_2	0.0	-
Refractive Index of Unmodified Fiber Core	n_{co}	1.46	-
Refractive Index of the Gain Medium	n_1	3.3	-
Total Internal Loss	α_{int}	25	cm^{-1}
Linewidth Enhancment Factor	α_h	2	
Confinement Factor	Γ	0.1	-
Nonradiative Recombination Coefficient	A	4×10^8	s^{-1}
Bimolecular Recombination Coefficient	B	1×10^{-10}	$cm^3 s^{-1}$
Auger Recombination Coefficient	C_A	10×10^{-29}	$cm^6 s^{-1}$
Carrier Lifetime	τ_n	0.8×10^{-9}	s
Transparancy Carrier Density	N_o	1.2×10^{18}	cm^{-3}
Reference Carrier Density for Refractive Index	N_{rf}	2×10^{18}	cm^{-3}
Mode-locking Frequency	f_m	2.5	GHz
DC Bias Current (For Linearly and Sinusoidally Chirped)	I_{dc}	6	mA
RF Current Amplitude (For Linearly Chirped)	I_{rf}	20	mA
RF Current Amplitude (For Sinusoidally Chirped)	I_{rf}	22	mA
Length of Laser Diode	L_l	2.5×10^{-12}	cm
Width of the Laser Diode	w	1×10^{-4}	cm
Thickness of the Laser Diode	D	5×10^{-6}	cm
Operating Wavelength	λ	1.55×10^{-4}	cm
Speed of the Light in the Vacuum	c_o	3×10^{10}	cm/sec
Lenght of Grating*	L	4	cm
Length of Fiber*	L_f	2.06	cm
Effective Cavity Length	L_{eff}	4.06	cm
*: For 2.5 GHz			

3.2   Noise in the Laser

"Noise" of lasers is a short term for random fluctuations of various output parameters. Laser diodes are intrinsically noisy devices because of the quantum nature of the light. Even if when the laser is biased at a constant current, with negligible fluctuations, the output of a semiconductor laser exhibits fluctuations in its phase and in its intensity. These laser noise fluctuations are known as langevin noise forces that described the fluctuations of a system. Langevin noise term is to determine the quantum nature of the photon absorption and emission process. They play important roles to determine the linewidth and amplitude fluctuations of semiconductor laser. Spontaneous emission and electron-hole recombination, that one known as shot noise are two fundamental noise mechanisms. The fluctuations in carrier number result from the process of generation and recombination. Spontaneous emission results from a sum of contributions from throughout the laser. In the next sections, types of the noise in the laser which are spontaneous, carrier and RIN, will be discussed.

3.2.1   Spontaneous Emission Noise

Spontaneous emission occurs in all media. It is a phenomenon that can be understood in two different ways as follows. (1) Phenomenologically, the blackbody radiation is spontaneous emission in thermal equilibrium. Therefore, one can find out the spontaneous emission rate from the known blackbody radiation intensity. (2) In the quantized field theory, both the radiation field and the atomic particles are quantized. The radiation field is expressed as a superposition of modes and the number of photons in each mode, while the ψ (wave function) of atomic particles are expressed as summations of energy eigen states with probability meaning for the coefficient of each state. The interaction between the radiation field and the atomic particles is expressed as the annihilation and creation of photons in each mode, while changes in the coefficients of the atomic energy states signify the change in energy of the atomic particles. The downward transition of the atomic particle can be induced by any radiation mode, even when there is no photon in that mode. This means that, in this case, radiation is emitted into all the modes in the absence of the photon in the radiation field [54]. This is the theoretical basis for spontaneous emission.

In addition, radiation is emitted or absorbed from these modes that have photons. This is the basis for induced transition. In phenemoligical analysis, the effect of spontaneous emission might be include in the rate equation anlysis of the lasers. In this case of the laser oscillators, the spontaneous emission produces phase noise that is the origin of the minimum linewidth of the laser output. It also produces an amplitude fluctuation that is the origin of the relative intesity noise.

Fluctuations can effect the performance of the lightwave systems therefore it is important to estimate their magnitude. As seen in the Fig. 3.1, it has two parts; imaginary part causes the phase fluctuations and real part causes the amplitude fluctuations.
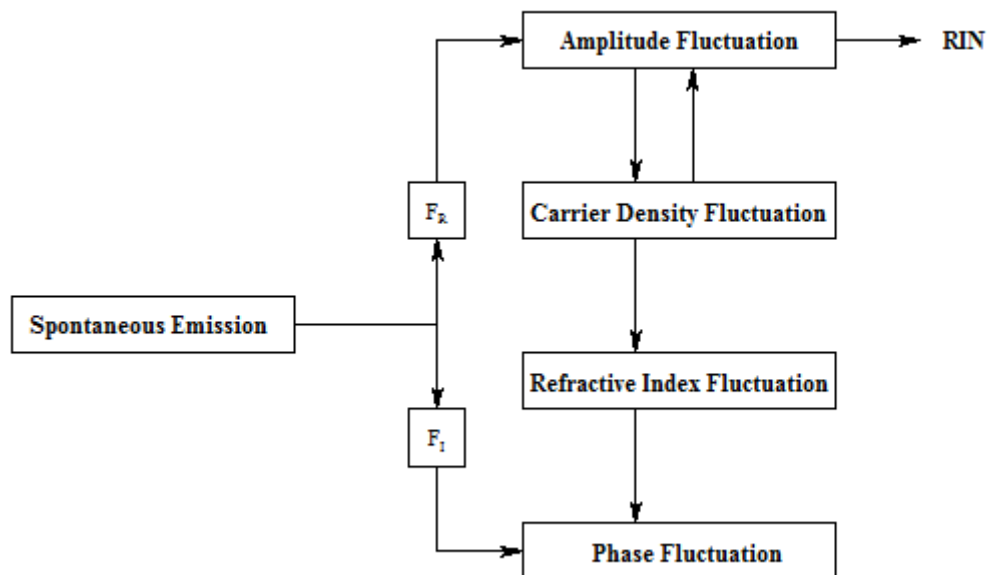
Figure 3.1 Noise diagram in laser [26]

As seen in Fig.3.1, spontaneous emission perturbs both amplitude and phase fluctuation in a random manner. The immaginary part F_I causes the phase fluctuations, and the real part F_R causes the amplitude fluctuations. The small fluctuations in amplitude lead to small fluctuations in the carrier density. In the figure, there are two mechanisms contribute to the phase fluctuations. The first mechanism is the imaginary part of the spontaneous emission. Each spontaneously

emitted photon changes the optical phase by a random amount. In the second mechanism, fluctuations in the carrier populations also lead to a phase change. These fluctuations can affect the performance of lightwave systems, and it is important to estimate their magnitude [8, 34, 36]. The laser cavity is divided into equal M_L sections with $\Delta z = v_g \Delta t$. For each time step, the fordward and backward fields are calculated from the transfer matrix. In each section of the laser, the carrier density is calculated from the rate equation as,

$$\frac{dN(z,t)}{dt} = \frac{I(t)}{eV} - \frac{N(z,t)}{\tau_n} - \frac{a_o(N(z,t) - N_o)}{1 + \varepsilon S(z,t)} v_g S(z,t) + F_N \qquad (3.1)$$

where I(t) is the injection current, V is the active layer volume, e is the electron charge, N(z,t) is the carrier density, τ_n is the carrier life time, S(z,t) is the photon density, N_o is the carrier density at tranparency, ε is the gain saturation parameter, and a_o is the differential gain. The semiconductor is active, including gain of the form $\Gamma a_o(N(z,t)-N_o)/(1+\varepsilon S(z,t))$, where Γ is the optical confinement factor.

3.2.2 Carrier Noise

The carrier noise F_N results from two kinds of process and can be written in the following way [38]

$$F_N(z,t) = F_{nr}(z,t) - F_s(z,t) \qquad (3.2)$$

The first term F_{nr} on the right-hand side of Eqn. 3.2 describes the noise of the injection current and the noise caused by nonradiative recombination of carriers. This noise term is not correlated with the process of spontaneous emission and represents Gaussian white noise with correlation [36].

$$< F_{nr}(z,t) F_{nr}(z',t') > = (I/eV + N/\tau_n)\delta(t-t')\delta(z-z') \qquad (3.3)$$

Here, the first term determines the noise of the injection currents; it is neglected in this analysis. The second term F_s on the right-hand side of Eqn. 3.2 results from

radiative recombination and is therefore correlated with the spontaneous emission and it is proportional to the fluctuation of the optical intensity.

The autocorrelation for $F_N(z,t)$ and the cross correlation between $F_N(z,t)$ and $s(z,t)$ become,

$$< F_N(z,t)F_N(z^{'},t^{'}) > = (I/qV + N/\tau_n + \frac{a_0(N-N_0)}{1+\varepsilon P}v_g P)\delta(t-t^{'})\delta(z-z^{'}) \qquad (3.4)$$

and

$$< F_N(z,t)s(z^{'},t^{'}) > = (-\beta_{sp}R_{sp}\frac{a_0(N-N_0)}{1+\varepsilon P}P)\delta(t-t^{'})\delta(z-z^{'}) \qquad (3.5)$$

3.3 Relative Intensity Noise (RIN)

The study of noise in lasers began with work by Mc. Cumber [54], where the rate equations are modeled with the inclusion of Langevin noise terms. A study of noise begins with a clear understanding of the Langevin noise terms introduced in the rate equations. Noise in lasers is due to the discrete nature of the electrons and photons inside the cavity. Each change in the photon or electron number is a random event with a probability of the event occurring.

There are fluctuations of laser intensity cause by random spontaneous emissions. This fluctuation is known as relative intensity noise. In other words, RIN can be tought of as a type of inverse carrier-to-niose-ratio and it can be defined as,

$$\frac{RIN(f)}{\Delta f} = \frac{2 < |\Delta S(\omega)|^2 >}{< S >^2} \qquad (3.6)$$

where $RIN/\Delta f$ is in dB/Hz, $<S>$ is the average optical power, $\Delta S(\omega)$ is the spectral density of noise in a Δf bandwidth at a specified frequency. Note that effective bandwidth is $2\Delta f$ since it must include both positive and negative frequencies.

The relative intensiy noise spectrum is not flat as the spectrum for white noise. The RIN is frequency dependent. However, for simplicity, most connection analysis

assume that RIN is constant within the bandwidth of interest. The RIN also differs for diode and solid state lasers and for single mode and multiple mode lasers. For example, single-mode solid state lasers may have a RIN of −170 dB for $1f = 1$ Hz, whereas diode lasers typically have a RIN of −145 dB for $1f = 1$ Hz. [59].

3.4   Mode-Locked HSPS Results for Sinusoidally Chirped FBG

In this section, the output of the mode-locked HSPS is given with and without noise for sinusoidally chirped FBG. DC and RF currents applied to the laser diode are 6 and 22 mA for sinusoidally chirped FBG, respectively. The pulsewidth and spectralwidth are determined in order to calculate the TBP of the pulses.

Transform limited pulses from mode-locked HSPS with sinusoidally chirped Gaussian-apodized FBG are obtained over a wide tuning range 1.1 GHz (2.1-3.2 GHz) around the fundamental mode-locking frequency without noise, with spontaneous noise, carrier noise and both spontaneous and carrier noise. As shown in Fig. 3.2, an output pulse is produced without noise which has pulsewidth of 39.343 ps, TBP of 0.366, and spectralwidth of 9.299 GHz at the fundamental mode-locked frequency of 2.5 GHz.
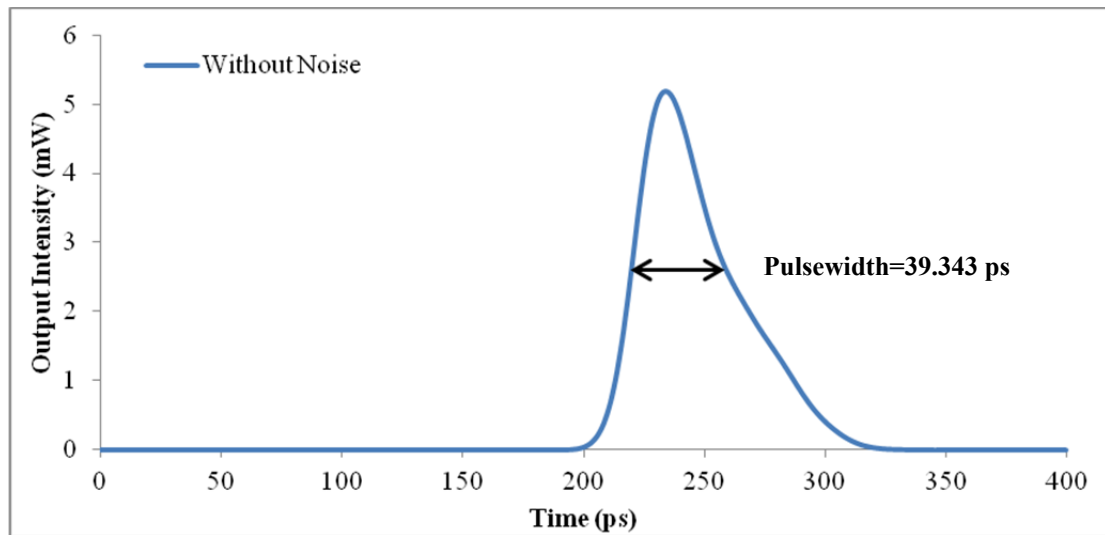
Figure 3.2 Output intensity spectrum of mode-locked HSPS for sinusoidally chirped Gaussian apodized FBG without noise at the mode-locking frequency of 2.5 GHz.

The output pulse with spontaneous noise which has a pulsewidth of 39.068 ps, TBP of 0.375, spectralwidth of 9.588 GHz and RIN of -126.811 dB/Hz at the

fundamental mode-locking frequency of 2.5 GHz is shown in Fig. 3.3. However, TBP is in the range of 0.3-0.5, transform-limited pulse is not generated because the number of peak in the frequency and field spectra are not equal to one. Although transform limited pulse is not generated, RIN is decreased when it is compared to the linearly chirped Gaussian-apodized FBG and the value of RIN is -114.209 dB/Hz for linearly chirped Gaussian-apodized at the fundamental mode-locking frequency of 2.5 GHz. The peak power of sinusoidally chirped Gaussian-apodized FBG is 5.252 mW and 5.039 mW for linearly chirped Gaussian-apodized FBG.

If carrier noise is considered, in this case, transform limited pulse is again not generated at fundamental mode-locking frequency of 2.5 GHz because the value of TBP is 0.007 as shown in Fig. 3.3.
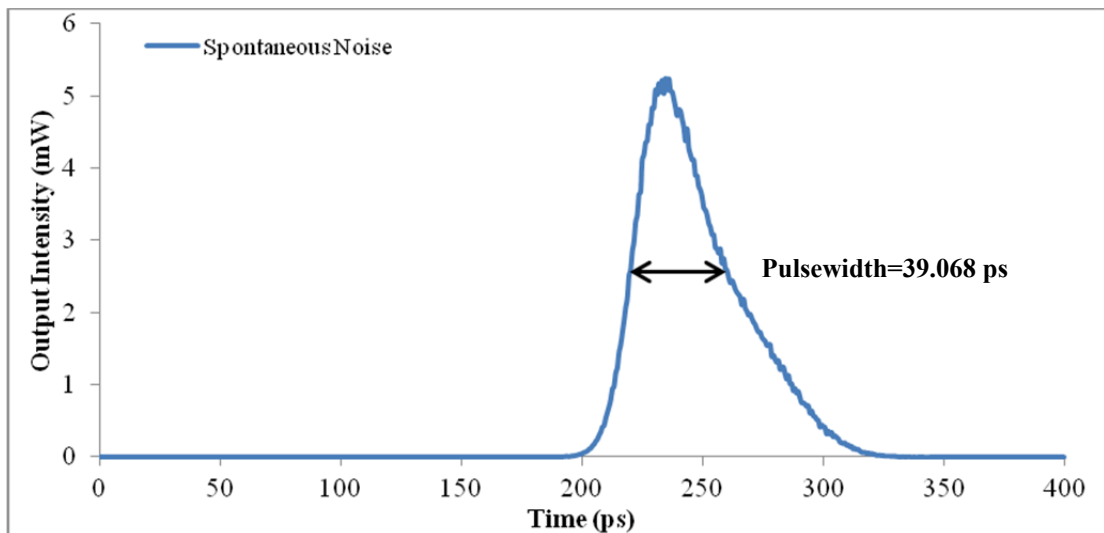
Figure 3.3 Output intensity spectrum of mode-locked HSPS for sinusoidally chirped Gaussian apodized FBG with spontaneous noise at the mode-locking frequency of 2.5 GHz.

Also, as seen in Figure 3.4, pulsewidth is 0.827 ps, spectralwidth of 8.725 GHz, the peak power of 7.527 mW and RIN of -98.241 dB/Hz for sinusoidally chirped and pulsewidth is 47.192 ps, spectralwidth of 8.648 GHz, the peak power of 4.368 mW and RIN of -113.816 dB/Hz for linearly chirped Gaussian-apodized FBGs. If the results are compared with spontaneous noise for both types of chirped, it is easy to understand of the effect of the carrier noise in the system.
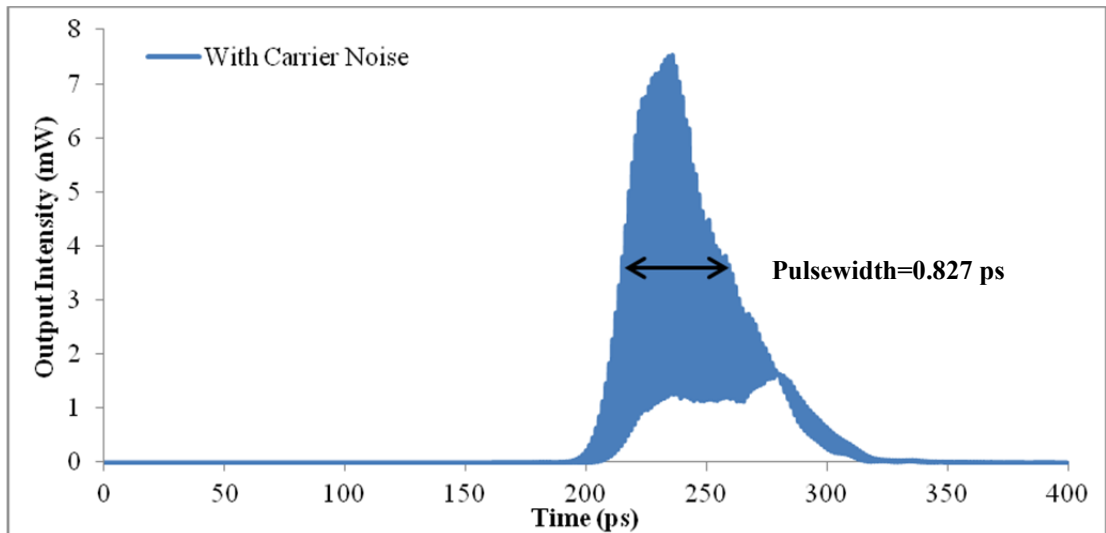
Figure 3.4 Output intensity spectrum of mode-locked HSPS for sinusoidally chirped Gaussian apodized FBG with carrier noise at the mode-locking frequency of 2.5 GHz.

When both spontaneous and carrier noise are taken into account then the output intensity spectrum will be as shown in Figure 3.5. Transform limited pulses are generated only between 2.6 and 3 GHz (400 MHz). Since at 2, 2.1, 2.3 and 3.1 GHz, the TBP is smaller than 0.3 and at 2.2 and 2.4-2.5 GHz , the field spectra is not equal to one, therefore, transform limited pulses are not generated at these mode-locking frequencies as shown Fig. 3.5.
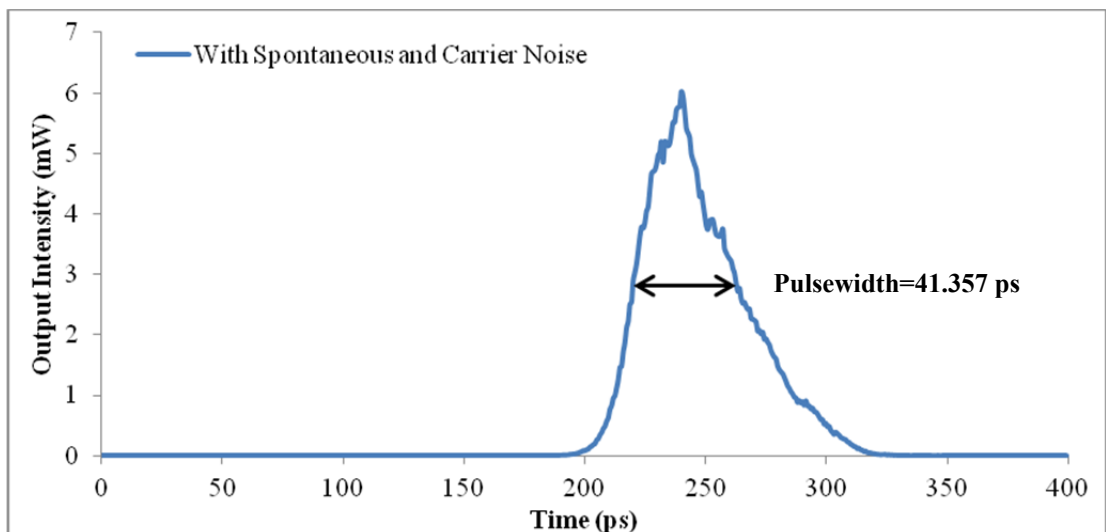
Figure 3.5 Output intensity spectrum of mode-locked HSPS for sinusoidally chirped Gaussian apodized FBG with spontaneous and carrier noise at the mode-locking frequency of 2.5 GHz.

Also, as seen in the Fig. 3.5, pulsewidth is 41.357 ps, spectralwidth of 9.805 GHz, the peak power of 6.034 mW and RIN of -112.544 dB/Hz for sinusoidally chirped and pulsewidth is 1.278 ps, spectralwidth of 8.803 GHz, the peak power of 8.284 mW and RIN of -102.903 dB/Hz for linearly chirped Gaussian-apodized FBG.

The TBP was calculated as the product of the pulsewidth and spectralwidth. The program which was used in the simulation, calculated all the parameters for 500 round trips, and the results are taken for every 100th round trip to observe whether a regular pulse train was generated or not [8, 34-36]. The simulation results show that the transform-limited pulses were produced for a wider frequency range (2.1-3.2 GHz) 1.1 GHz.

Mode-locking characteristics of an HSPS utilizing a sinusoidally chirped Gaussian-apodized FBG were investigated without noise by Dogru [34]. Results showed that transform-limited pulses generated for a wider frequency range 2.1-3.2 GHz (1.1 GHz), when the standard parameters were used in Table 3.1 [8]. The pulsewidth and TBP as a function of mode-locking frequency are shown in Fig. 3.6. The value of TBP is in the range of the transform limited (0.3-0.5).
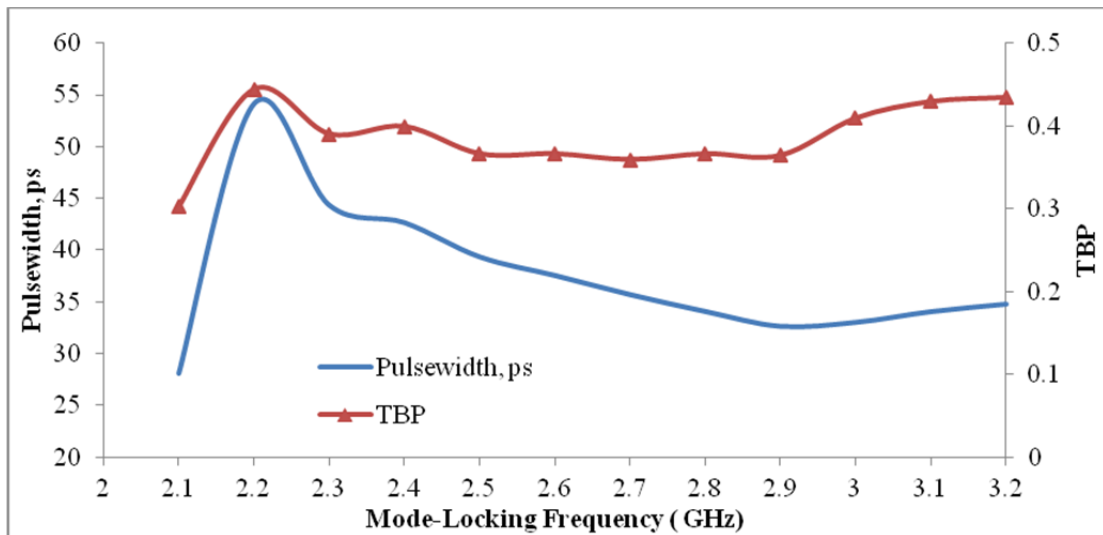
Figure 3.6 Pulsewidth and TBP as a function of mode-locking frequency without noise.

If both spontaneous and carrier noise are taken into system, some value of TBP getting out of the transform-limited range where mode-locking frequencies are 2, 2.1 and 3.1 GHz as shown in Fig. 3.7.
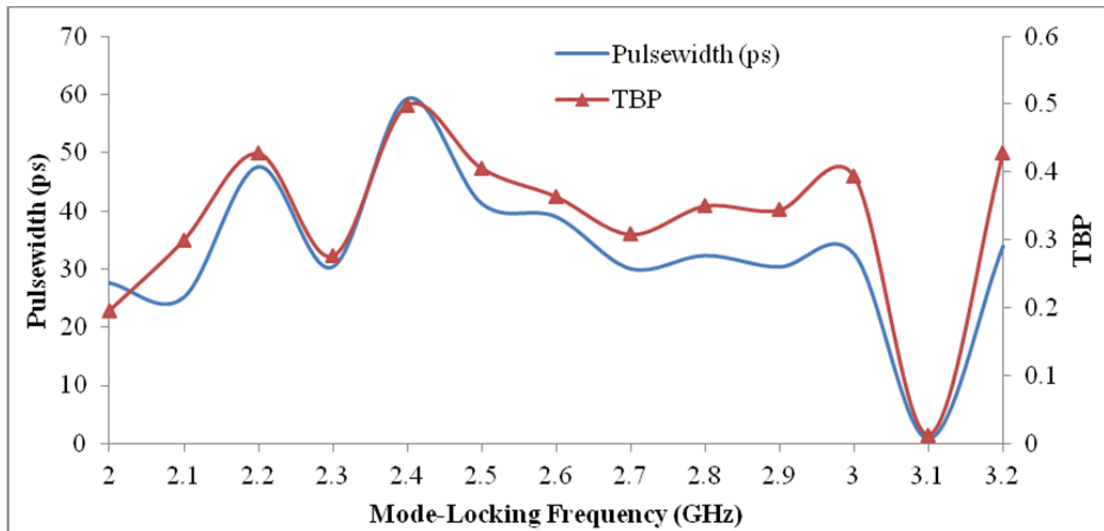
Figure 3.7 Pulsewidth and TBP as a function of mode-locking frequency with both spontaneous and carrier noise.

Transform limited pulses are generated between 2.6 and 3 GHz. In addition, it can be easily understood in the Figure 3.7 that pulsewidth is inversely proportional to with the spectralwidth or vice versa, because TBP is product of the pulsewidth and spectralwidth.
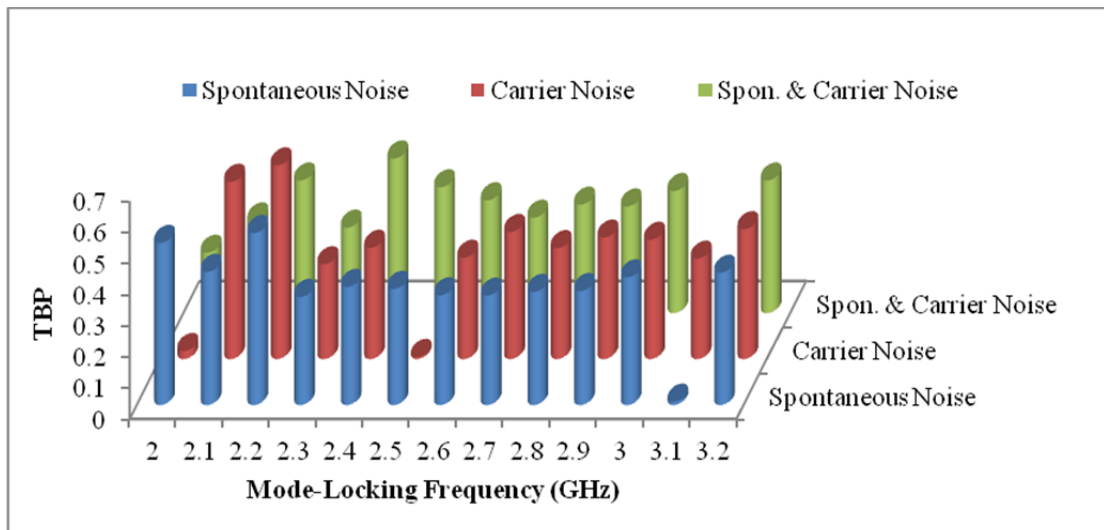
Figure 3.8 TBP as a function of mode-locking frequency with spontaneous noise, carrier noise and both spontaneous and carrier noise.

Figure 3.8 shows the TBP as a function of mode–locking frequency with spontaneous, carrier and both spontaneous and carrier noise. It was observed in the figure that when only carrier noise is applied into the system then TBP goes out of the range and RIN increases with carrier noise. RIN has a peak (-98.241 dB/Hz) at

the fundamental frequency of 2.5 GHz where the pulse is not transform-limited, giving a TBP of 0.007 as seen in Fig. 3.8. Transform limited pulses are generated only 2.6-3.1 GHz.

As seen in these results, carrier noise affects the output pulse of the mode-locked HSPS as much as spontaneous noise.

The pulsewidth as a function of mode-locking frequency for linearly chirped and sinusoidally chirped FBGs are shown in Fig. 3.9 when both spontaneous and carrier noise are taken into account. It can be observed in the figure that, except at the mode-locking frequency of 2.4 GHz, the pulses generated with the sinusoidally chirped grating are shorter than those generate with the linearly chirped grating.
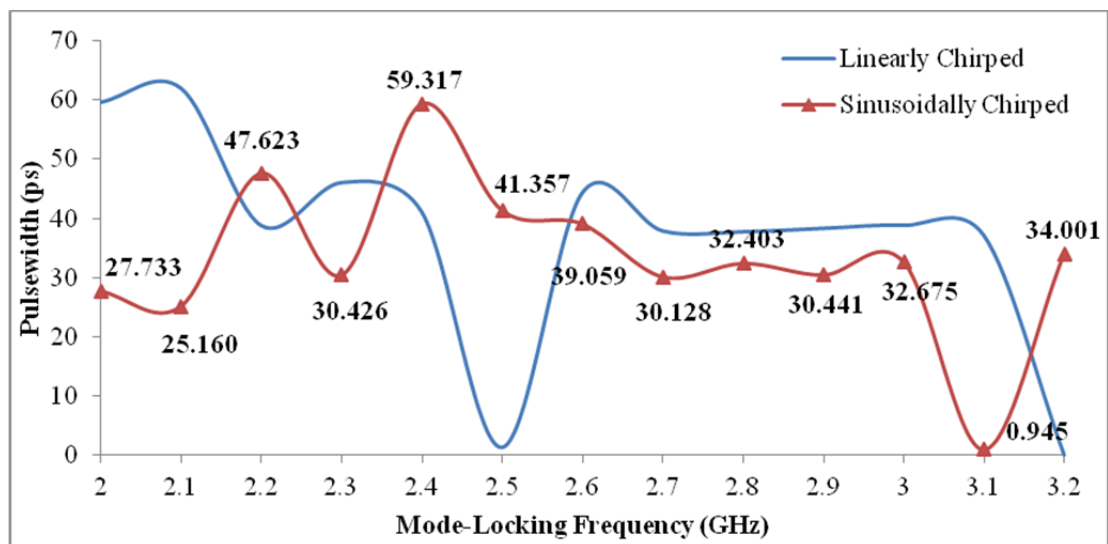
Figure 3.9 Pulsewidth as a function of mode-locking frequency for Linearly chirped and Sinusoidally chirped with both spontaneous and carrier noise.

In the Fig. 3.10, TBP as a function of mode-locking frequency for Linearly chirped and Sinusoidally chirped FBGs are shown when both spontaneous and carrier noise are taken into account. The value of the TBP is in the range of 0.3-0.5 for most of mode-locked frequencies except 2, 2.1, 2.3 and 3.1 GHz when the chirp is sinusoidal and the value of TBP for sinusoidally chirped are shown on the bar graph. On the other hand, transform limited pulses are generated only 2 - 2.1 and 2.6 - 3 GHz for linearly chirped Gaussian apodized. Consequently, it can be said, transform-limited pulses are generated when mode-locking frequencies are increased.
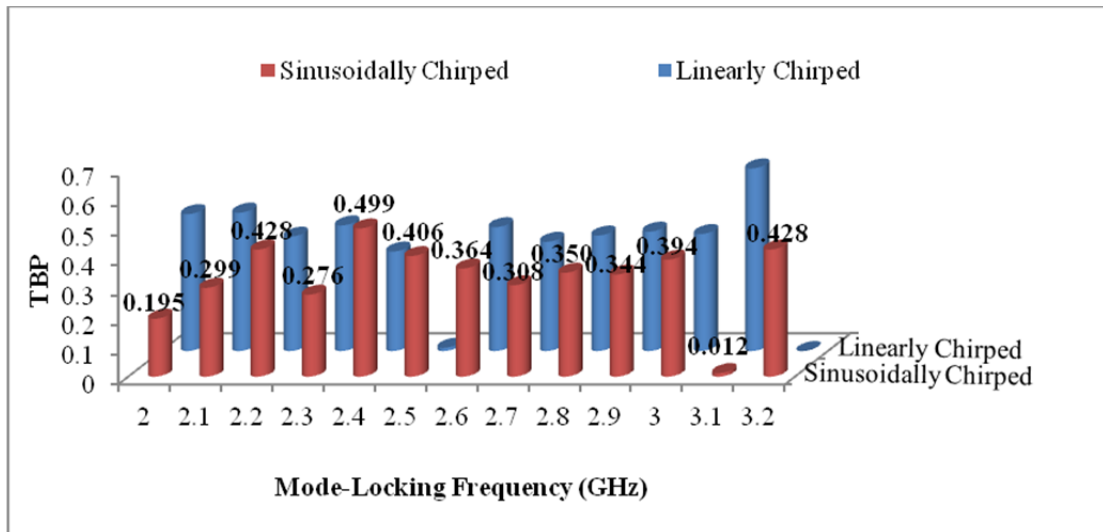
Figure 3.10 TBP as a function of mode-locking frequency for Linearly chirped and Sinusoidally chirped with both spontaneous and carrier noise.

CHAPTER 4

RELATIVE INTENSITY NOISE (RIN) OF HSPS

4.1   Introduction

In this chapter, RIN of HSPS for sinusoidally chirped Gaussian apodized FBG will be described and the most effective noise terms will be determined through the results. In our simulation the cross correlation between the carrier and spontaneous noise is neglected because of the effect of this noise on RIN is very little.

4.2   Relative Intensity Noise (RIN) of   HSPS for Sinusoidally Chirped Gaussian Apodized FBG

In this section, effect of the spontaneous and carrier noise on RIN will be described for sinusoidally chirped Gaussian apodized FBGs for a wide frequency range of 1.2 GHz (2-3.2 GHz) around the fundamental frequency of 2.5 GHz.

Figure 4.1 shows RIN of HSPS for sinusoidally chirped Gaussian apodized FBG with spontaneous noise, carrier noise and both spontaneous and carrier noise where wavelength of the laser 1550 nm, chirp coefficient C= $-45*10^8$ A $\%$/cm and the other standard laser and grating parameters were given in Table 3.1 at fundamental frequency of 2.5 GHz [32-36].

As seen in Fig. 4.1, there is not a RIN peak between 2.4 and 3 GHz when spontaneous and both spontaneous and carrier noise are taken into system but RIN spectrum had a peak at the fundamental frequency of 2.5 GHz when only carrier noise is taken into account. However, the RIN spectrum had a peak at the fundamental frequency for all three noise conditions for linearly chirped Gaussian apodized FBG which was investigated by Dogru *et. al* [8, 50-51]. Transform limited pulses are generated only at the mode-locking frequency of 2.1 GHz and between 2.6 and 3 GHz (400 MHz) with only spontaneous noise as seen in Fig. 4.1.
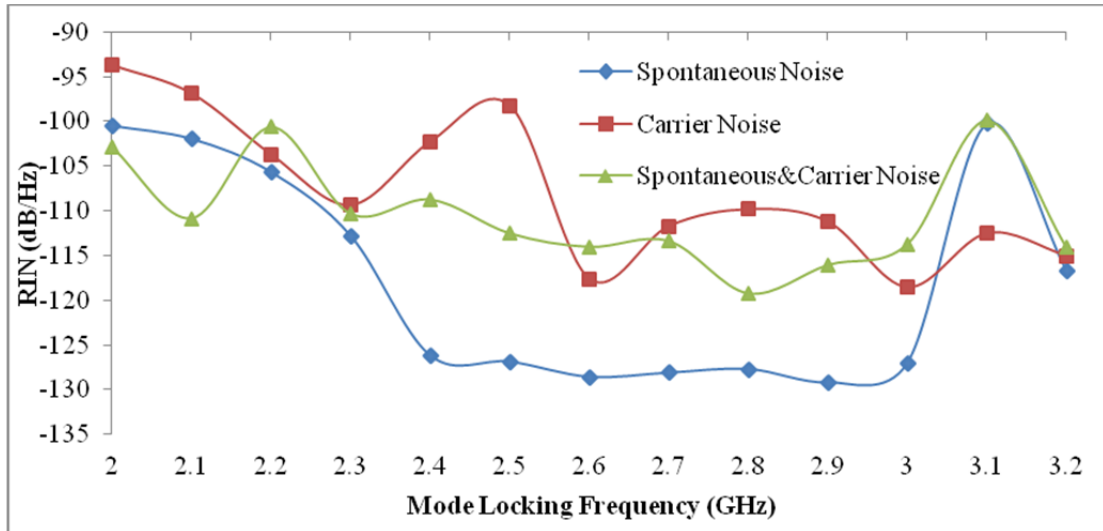
Figure 4.1 RIN Spectrums of HSPS for Sinusoidally Chirped Gaussian Apodized FBG.

The fundamental frequencies of 2 and 2.2 GHz are not transform limited pulse because the TBPs are greater than 0.5 and at 3.1 GHz, the TBP is 0.011 because of this reason transform limited pulse is not generated as given in Fig. 4.1. When both noises taken into system then transform limited pulses are generated only between 2.6 and 3 GHz (400 MHz). Because at 2, 2.1, 2.3 and 3.1 GHz, the TBPs are smaller than 0.3. Although, at 2.4-2.5 and 3.2 GHz, TBPs are lying in the range of 0.3 and 0.5, again transform limited pulses are not generated because the number of the peak in the frequency and field spectra are not equal to one. If only carrier noise taken into system, then the RIN spectrum has a peak where the value is -98.241 dB/Hz at the fundamental frequency of 2.5 GHz and transform limited pulse is not generated because of giving a TBP of 0.007 as seen in Fig. 4.1. Transform limited pulses are produced at fundamental frequencies of 2.6-3.1 GHz (500 MHz). All these results showed that carrier noise is also effective on the output pulses of the mode-locked HSPS as much as the spontaneous noise.

If both spontaneous and carrier noise are added in the HSPS system, a decrease in the RIN occurs as indicated in Fig. 4.1 when the result is compared with that of carrier noise. The peak decreases 14.3 dB and the peak value of the RIN decreases from -98.241 dB/Hz to -112.544 dB/Hz. Transform limited pulses are generated again 2.6-3 GHz (400 MHz).

4.3 Effects of RF and DC Currents on RIN of HSPS

In this section, effects of RF and DC currents on RIN characteristics of HSPS with sinusoidally chirped Gaussian apodized FBGs including both spontaneous and carrier noise will be presented. For this purpose, the ranges are taken 2-3.2 GHz for the frequency, 10-30 mA with 5 mA steps and 4-8 mA with 1 mA steps for the RF and DC currents, respectively [32-36]. RF current range also includes 22 mA, because this value is the optimum value for sinusoidally chirped.

4.3.1 Effects of RF and DC Currents on RIN of HSPS Utilizing Sinusoidally Chirped Gaussian Apodized FBG

In order to investigate the effects of the level of the RF current, the laser diode is biased at a constant DC bias of 6 mA. The magnitude of the RF current is changed between 10 and 30 mA with 5 mA steps. RF current also includes 22 mA, because the value is the optimum value for sinusoidally chirped.

If RF current increases, RIN peak shifts from 2.5 GHz to lower frequencies and also there is a peak for all RF currents at mode-locked frequency of 3.1 GHz as shown in Fig. 4.2 with spontaneous noise. At 3.1 GHz, the value of TBP is 0.011 when RF currents are 22 and 25 mA, and the value of TBP is 0.012 for RF current which value is 20 mA. For the other RF currents, the value of TBP is 0.013, transform limited pulses are not generated as shown in Fig 4.2. Transform limited pulses are generated at the mode-locking frequencies 2.6-3 GHz for all RF currents and at this time, the RIN peaks are approximately same. The same condition was also reported by Dogru [8] for Linearly chirped Gaussian-apodized FBGs.

At mode-locking frequencies of 2.3 - 2.5 and 3.2 GHz, the values of TBP are in the range of 0.3-0.5, and the RIN values are -100.439, -119.477, -120.202, -125.981 and -116.975 dB/Hz, respectively when RF current is 22 mA which is the standard parameter for sinusoidally chirped Gaussian-apodized FBG.
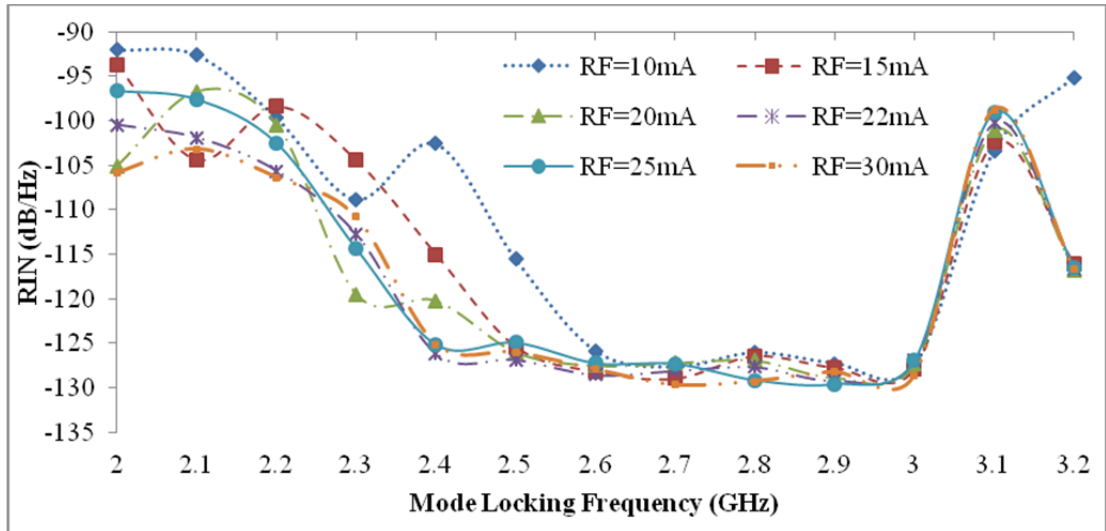
Figure 4.2 RIN Spectrums of HSPS for Sinusoidally Chirped Gaussian Apodized FBG including Spontaneous Noise with different RF current for a DC current of 6 mA.
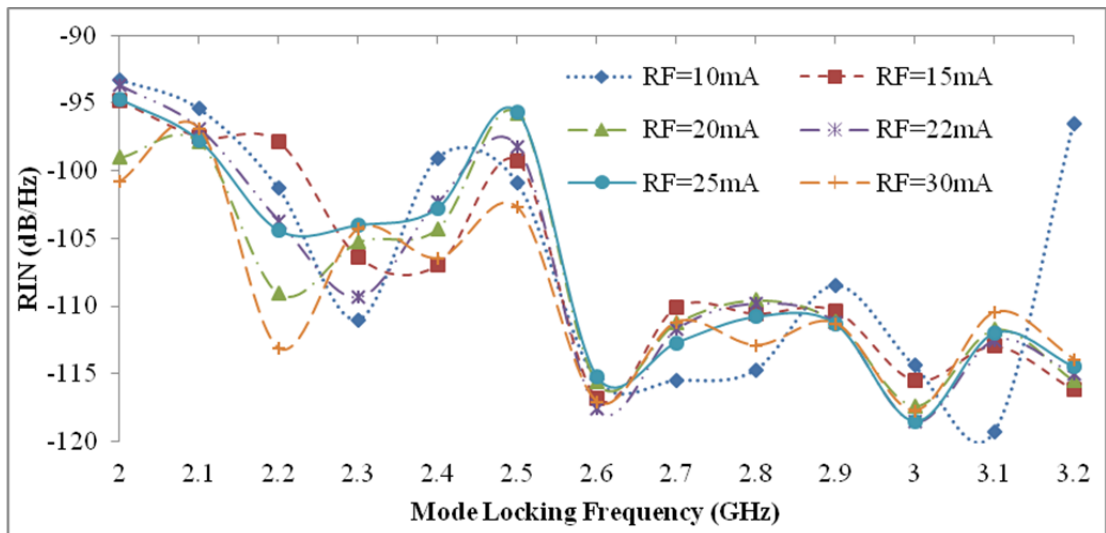
Figure 4.3 RIN Spectrums of HSPS for Sinusoidally Chirped Gaussian Apodized FBG including Carrier Noise with different RF current for a DC current of 6 mA.

RIN spectrums of HSPS for sinusoidally chirped Gaussian-apodized FBG including carrier noise with different RF current for a DC current of 6 mA as shown in Fig 4.3. From 22 mA, increase or decrease the RF flow, causes an increase in the relative-intensity noise. If it is compared with when only spontaneous noise is taken into the account, it is seen clearly from the Fig. 4.3, the relative-intensity noise decreases. The transform limited pulses are generated between 2.6-3.1 GHz (500MHz) for all RF currents except the value of 30 mA, at this case, transform limited pulses are

obtained between 2.6 and 3 GHz (400 MHz). Although there is a peak at the fundamental frequency of 2.5 GHz for all RF currents, transform limited pulses are not generated since TBPs are out of the range which is 0.3-0.5.

Figure 4.4 RIN Spectrums of HSPS for Sinusoidally Chirped Gaussian Apodized FBG including Spontaneous and Carrier Noise with different RF current for a DC current of 6 mA.

Figure 4.4 shows effect of RF current on RIN if both of noise (spontaneous and carrier) is taken into account. In this case, transform limited pulses are generated at mode-locking frequencies between 2.6 and 3.1 GHz and also transform limited pulses are generated at mode-locked frequency of 2 GHz when the values of RF current are 25 and 30 mA.

Figure 4.5 shows the effect of the DC current on the RIN when the laser diode is driven with 22 mA of RF current at the fundamental mode-locking frequency of 2.5 GHz. The magnitude of DC current is changed between 4 mA and 7 mA with 1 mA steps.

As seen in Fig. 4.5, If DC current increases, relative-intensity noise (RIN) is also increase. In this case, transform limited pulses are obtained for all DC current between 2.6-3 GHz with only spontaneous noise including the account and the RIN values are approximately same. Transform limited pulses are also obtained at mode-locking frequencies of 2 and 2.1 GHz for a current 5 mA and 2,1 GHz for 6 mA and 2 GHz for 4, 7, 8 mA.

Figure 4.5 RIN Spectrums of HSPS for Sinusoidally Chirped Gaussian Apodized FBG including Spontaneous Noise with different DC current for a RF current of 22 mA.

For DC curent of 6 mA, at the mode-locking frequencies of 2.3, 2.4, 2.5 and 3.2 GHz the value of the TBP is in the standard range but transform limited pulses are not generated because of the side lobes. Although there is a peak at the mode-locking frequency of 3.1 GHz, transform limited pulse is not obtained because in this case TBP becomes 0.011.

If carrier noise is considered, the RIN increases when the DC currents increase. The mode-locking range where transform limited pulses are generated as seen in Fig. 4.6 is 600 MHz for a DC current of 6 mA. Transform limited pulse is not generated at fundamental mode-locking frequency of 2.5 GHz because the value of TBP is 0.007. Although the values of the TBP are in the range of 0.3-0.5 at the mode locking frequencies of 2.3, 2.4 and 3.2 GHz, transform limited pulses are not generated because the number of the peak in the frequency and field spectra are not equal to one.

Figure 4.7 shows the RIN spectrum of HSPS for sinusoidally chirped Gaussian-apodized FBG including both spontaneous and carrier noise with different DC current for a RF current of 22 mA. It is clear in the Fig 4.7, when DC current increases, RIN also increases. If Fig. 4.7 is examined carefully, it is found out 4, 5 and 6 mA of DC current is the best values for mode-locked HSPS because of giving 700 Mhz, 700 MHz and 500 MHz mode-locking range where transform limited pulses are generated, respectively.

But for the laser action the biased current must be selected above the threshold current (I_{th}).

The results show that the optimal value of RF current changes beween 20 and 25 mA with spontaneous noise and both spontaneous and carrier noise. Optimal DC current is 5 and 6 mA for all noises for mode-locked HSPS utilizing sinusoidally chirped Gaussian-apodized.
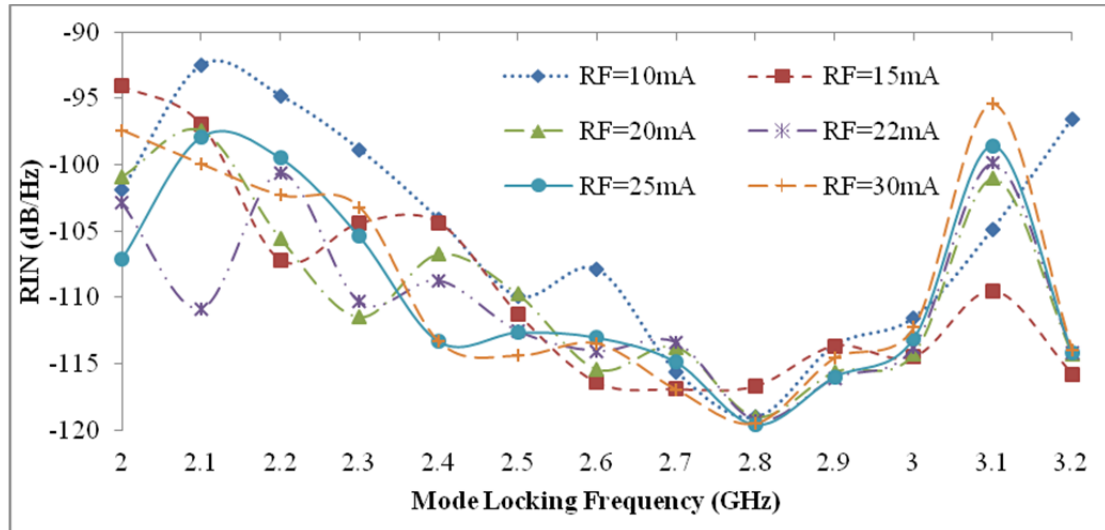

Figure 4.6 RIN Spectrums of HSPS for Sinusoidally Chirped Gaussian Apodized FBG including Carrier Noise with different DC current for a RF current of 22 mA.
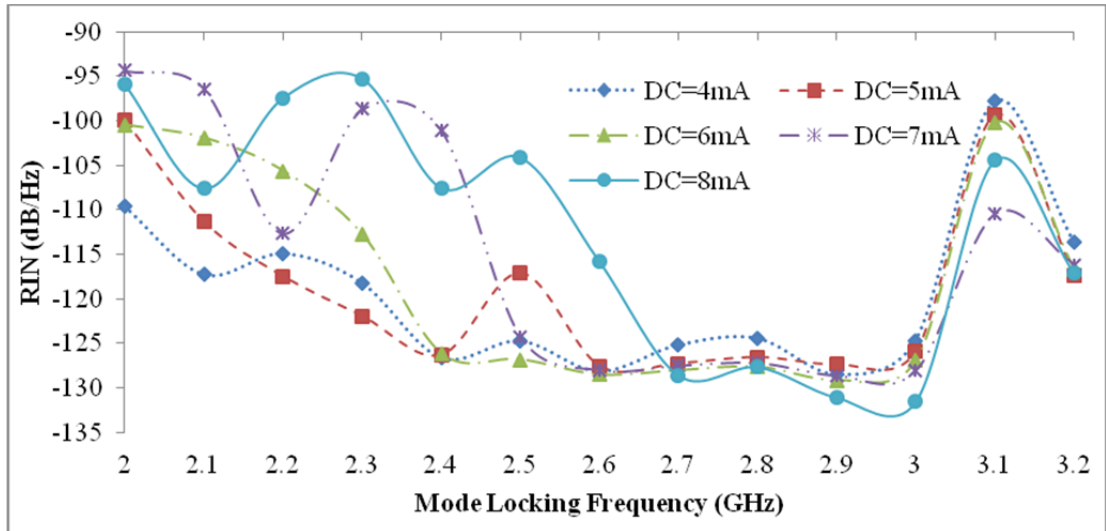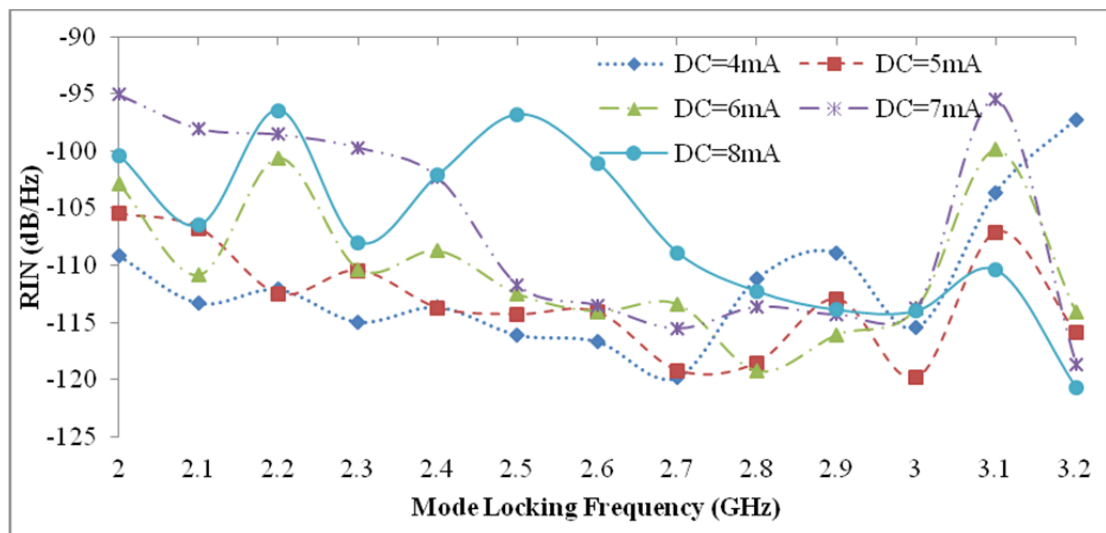

Figure 4.7 RIN Spectrums of HSPS for Sinusoidally Chirped Gaussian Apodized FBG including Spontaneous and Carrier Noise with different DC current for a RF current of 22 mA.
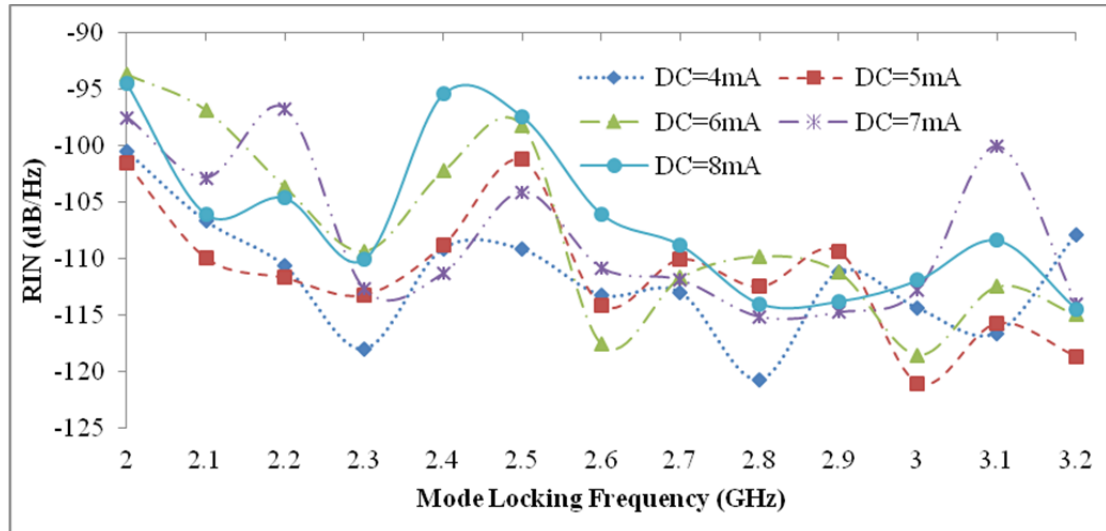
4.3.2 Conclusions

The numerical results indicated that the relative-intensity noise (RIN) is also extremely sensitive to DC and RF currents as shown before by Dogru *et al* [8]. for linearly chirped Gaussian-apodized FBG. The RIN increases with increasing DC current, and it also increase with decreasing values of RF current.

4.4 The Important Noise Parameters

In this section, we will try to determine the most effective noise parameters through the results. Simulations are made for sinusoidally chirped Gaussian apodized FBG when HSPS includes spontaneous noise and both spontaneous and carrier noise.

4.4.1 Linewidth Enhancement Factor

Essentially due to noise from spontaneous emission into the resonator modes, a free-running single-frequency laser has a certain finite linewidth. For simple cases, this fundamental limit for the linewidth was calculated by Schawlow and Townes even before the first laser was experimentally demonstrated. Whereas this limit was later shown to be closely approached by a number of solid-state lasers, significantly higher linewidth values were measured for semiconductor lasers (laser diodes) even when the influence of technical noise was very low. It was then later found by Henry that the increased linewidths result from a coupling between intensity and phase noise, caused by a dependence of the refractive index on the carrier density in the semiconductor. Henry introduced the ***linewidth enhancement factor α*** (also called *Henry factor* or *alpha factor*) [55-57] to quantify this amplitude–phase coupling mechanism; essentially, α is a proportionality factor relating phase changes to changes of the gain. It is possible to calculate the α factor of a semiconductor for a given carrier density from a band structure model, although this is not easy. For typical quantum wells, one often obtains values of the order to 2 to 5.

MQW lasers have α_h parameters that are about half those of similar lasers with bulk active layers and it is generally taken 2 for these lasers. For a semiconductor laser the refractive index depends on the carrier density and α_h determines this dependence. Although zero dependence is impossible to obtain in practice, in our simulation α_h is

varied 0 to 5. The effect of this parameter on the relative intensity noise (RIN) is given Fig. 4.8 and Fig. 4.9 for sinusoidally chirped Gaussian-apodized FBG. As seen in the Fig. 4.8, when α_h increases, RIN is also increase and transform limited pulses are generated at mode-locking frequencies between 2.6 – 3 GHz for α_h value of 2. At the fundamental frequencies of 2.2, 2.4, 2.5 and 3.2 GHz, the value of TBP is in the range of 0.3-0.5 but transform limited pulses are not generated because number of the field spectra is not equal to one. The transform limited pulses are generated for all mode-locking frequencies except 2 GHz when the noise is absent, in this case, TBP value of 0.281.
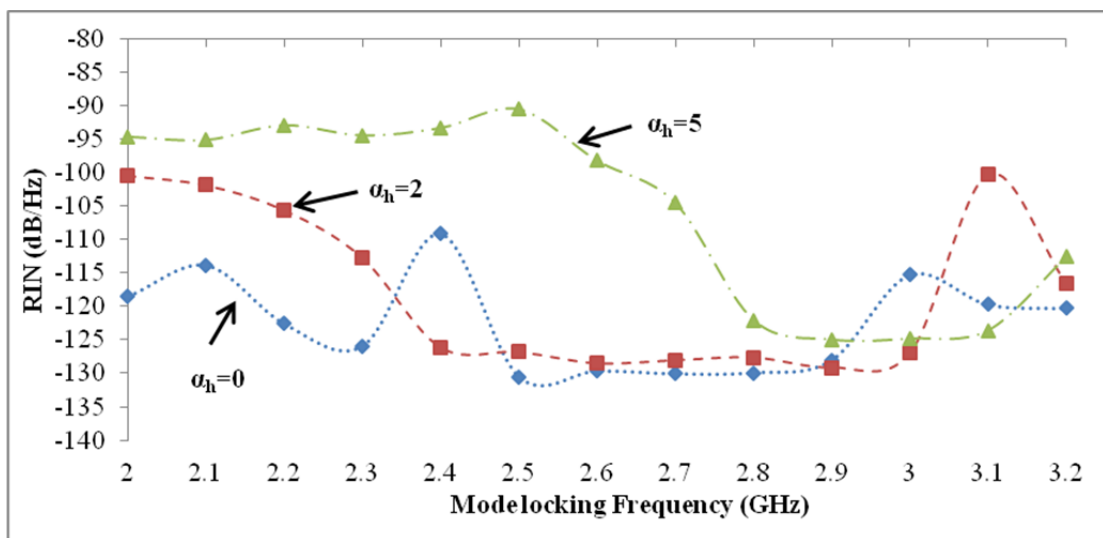
Figure 4.8 RIN Spectrums of HSPS with Sinusoidally Chirped Gaussian Apodized FBG for different α_h with Spontaneous Noise.
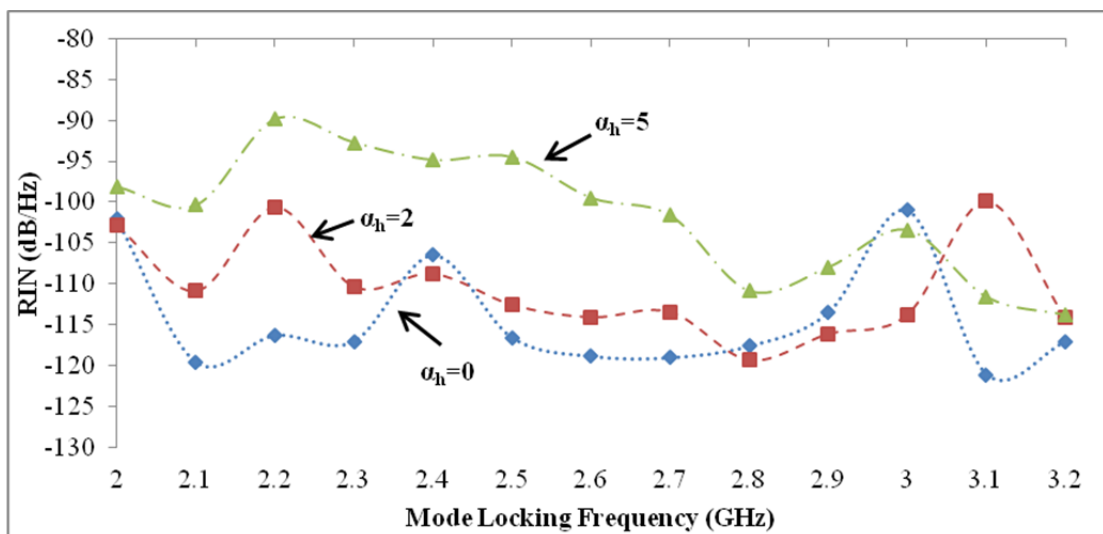
Figure 4.9 RIN Spectrums of HSPS with Sinusoidally Chirped Gaussian Apodized FBG for different α_h with both Spontaneous and Carrier Noise.

If both spontaneous and carrier noise are taken into account, transform limited pulses are again generated between 2.6 and 3 GHz for 2 value of α_h as shown in Fig. 4.9. RIN is low for its zero value but transform limited pulses are generated only at mode-locking frequencies of 2.4-2.6 and 2.9 GHz. For 5 values of α_h, transform limited pulse is obtained only at mode-locking frequency of 3 GHz.

Table 4.1 and 4.2 shows the variation in pulsewidth, spectralwidth and TBP for sinusoidally chirped Gaussian-apodized and linerly chirped Gaussian-apodized FBGs due to α_h at the fundamental mode-locking frequency of 2.5 GHz.

Table 4 1 Effects of varying α_h for sinusoidally chirped Gaussian-apodized FBG

α_h	Pulsewidth (ps)	Spectralwidth (GHz)	TBP
0	52.359[*]/51.613[**]/45.436[***]	10.276[*]/10.149[**]/10.222[***]	0.538[*]/0.524[**]/0.464[***]
2	39.343[*]/39.068[**]/41.357[***]	9.299[*]/9.588[**]/9.805[***]	0.366[*]/0.375[**]/0.406[***]
5	19.812[*]/0.774[**]/0.893[***]	9.900[*]/20.204[**]/7.365[***]	0.196[*]/0.016[**]/0.007[***]

Table 4 2 Effects of varying α_h for linearly chirped Gaussian-apodized FBG

α_h	Pulsewidth (ps)	Spectralwidth (GHz)	TBP
0	60.19[*]/60.17[**]/59.18[***]	9.42[*]/9.38[**]/9.41[***]	0.567[*]/0.564[**]/0.557[***]
2	45.38[*]/40.55[**]/1.278[***]	8.68[*]/8.60[**]/8.80[***]	0.394[*]/0.349[**]/0.011[***]
5	31.87[*]/41.77[**]/30.58[***]	10.98[*]/8.16[**]/11.26[***]	0.350[*]/0.341[**]/0.344[***]

*without noise   **with spontaneous noise   ***with both spontaneous and carrier noise

When α_h is changed between 0 to 5, the reduction in pulsewidths is very clear with and witohut noise for sinusoidally and linearly chirped Gussian-apodized FBG. However, there is a small increases at spectralwidth with α_h. TBP decreases with increasing α_h with and without noise for both sinusoidally and lineraly chirped Gaussian-apodized FBGs.

4.4.2 Gain Compression Factor

An amplifier device such as a laser gain medium cannot maintain a fixed gain for arbitrarily high input powers, because this would require adding arbitrary amounts of power to the amplified signal. Therefore, the gain must be reduced for high input powers; this phenomenon is called *gain saturation* (or *gain compression*). Gain compression (ε) is an important phenomenon for semiconductor lasers, especially InGaAsP based systems which exhibits very high gain compression. Gain compression caused several mechanisms such as spatial hole burning, spectral hole burning and other nonlinearities. Spatial hole burning can be neglected in high speed InGaAsP lasers due to the more dominant effect of the spectral hole burning. Spectral hole burning give rise power dependent gain.

Figure 4.10 and 4.11 shows the RIN of HSPS with sinusoidally chirped Gaussian-apodized FBG for different ε with spontaneous noise and both spontaneous and carrier noises are taken into account. At the standard parameter, transform limited pulses are generated over a wide frequency range of 2.1 - 3.2 GHz (1.1 GHz) without noises. When only spontaneous noise into the account, transform limited pulses are generated at mode locking frequency of 2.6 – 3 GHz for all values of ε. While ε increases, RIN also increases as shown in Fig. 4.10.
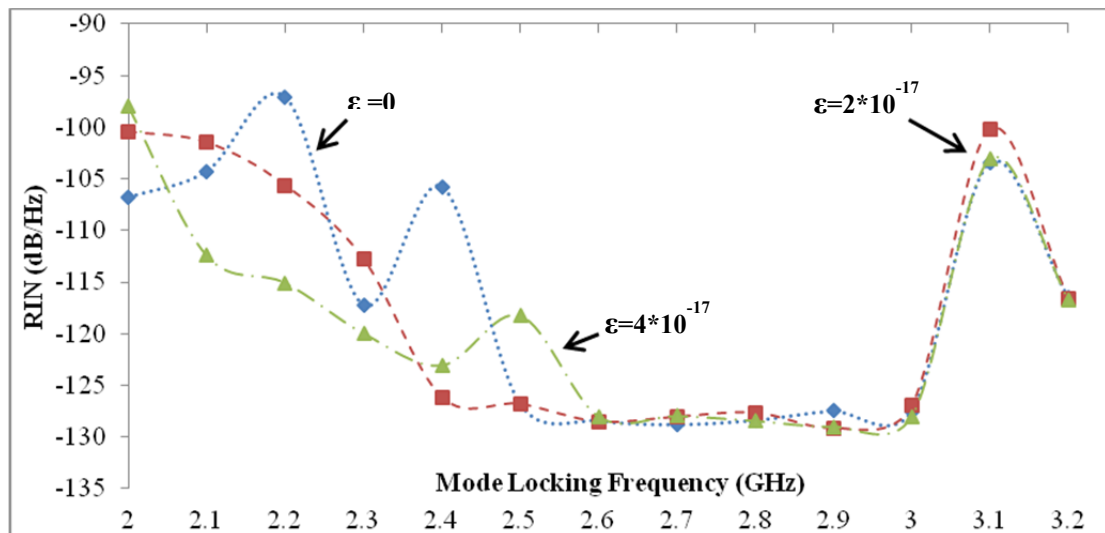
Figure 4.10 RIN Spectrums of HSPS with Sinusoidally Chirped Gaussian Apodized FBG for different ε with Spontaneous Noise.

If Fig 4.10 is examined, the value of $4*10^{-17}$ looks like more suitable for to be standard parameter but at the fundamental mode-locking frequency of 2.5 GHz, RIN value of $4*10^{-17}$ is higher than the RIN value of $2*10^{-17}$. In the Fig. 4.11, at the fundamental mode-locking frequency of 2.5 GHz, the value of the RIN are -111.619, -112.544, -110.116 dB when the values ε are 0, $2*10^{-17}$ and $4*10^{-17}$, respectively.
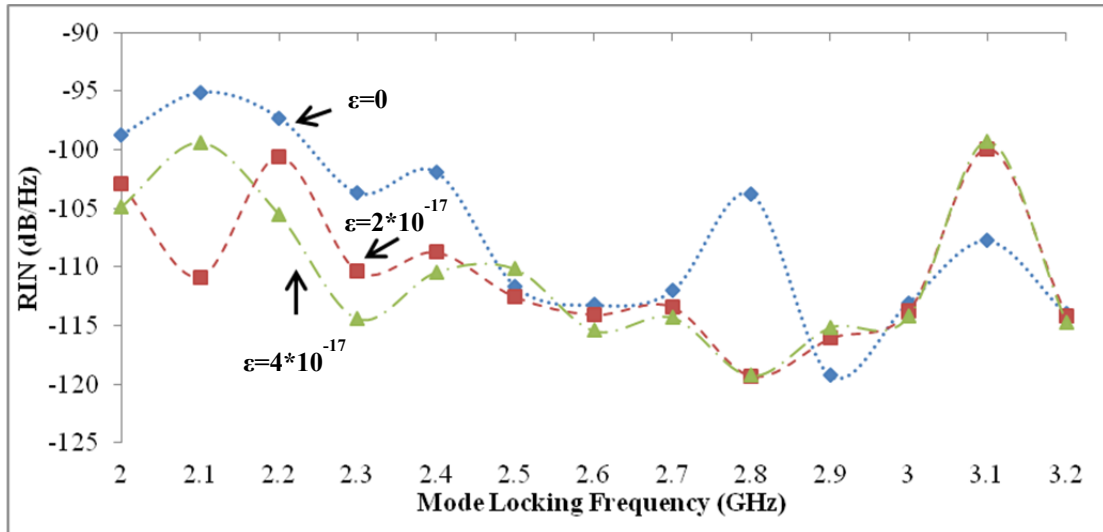
Figure 4.11 RIN Spectrums of HSPS with Sinusoidally Chirped Gaussian Apodized FBG for different ε with both Spontaneous and Carrier Noise.

Table 4.3 and 4.4 shows the variation in pulsewidth, spectralwidth and TBP for sinusoidally chirped and linearly chirped Gaussain-apodized FBGs due to ε at the mode-locking freqency of 2.5 GHz.

Table 4 3 Effects of varying ε for sinusoidally chirped Gaussian-apodized FBG

ε	Pulsewidth (ps)	Spectralwidth (GHz)	TBP
0	38.787[*]/39.110[**]/43.040[***]	9.276[*]/9.614[**]/9.403[***]	0.360[*]/0.376[**]/0.405[***]
$2*10^{-17}$	39.343[*]/39.068[**]/41.357[***]	9.299[*]/9.588[**]/9.805[***]	0.366[*]/0.375[**]/0.406[***]
$4*10^{-17}$	40.387[*]/39.594[**]/35.960[***]	9.517[*]/9.390[**]/9.671[***]	0.384[*]/0.372[**]/0.348[***]

*without noise   **with spontaneous noise   ***with both spontaneous and carrier noise

Table 4 4 Effects of varying ε for linearly chirped Gaussian-apodized FBG

ε	Pulsewidth (ps)	Spectralwidth (GHz)	TBP
0	44.630[*]/37.043[**]/0.937[***]	8.706[*]/9.043[**]/8.807[***]	0.389[*]/0.335[**]/0.008[***]
$2*10^{-17}$	45.381[*]/40.554[**]/1.278[***]	8.679[*]/8.604[**]/8.803[***]	0.394[*]/0.349[**]/0.011[***]
$4*10^{-17}$	46.107[*]/43.836[**]/17.846[***]	8.624[*]/8.636[**]/8.770[***]	0.398[*]/0.379[**]/0.157[***]

*without noise   **with spontaneous noise   ***with both spontaneous and carrier noise

As seen in the Table 4.3 pulsewidth, spectralwidth and TBP is slightly sensitive to ε with and without noises. Transform limited pulses are generated at the fundamental mode-locking frequency of 2.5 GHz without noises for all values of ε. Although TBP is in the range of 0.3-0.5 for all values of ε, transform limited pulses are not obtained with noise at the mode-locking frequency of 2.5 GHz.

Table 4.4 shows the effect of varying ε for linearly chirped Gaussian-apodized FBG with and without noise. It is found that although pulsewidth, TBP and spectralwidth are slightly sensitive to this parameter with spontaneous noise and without noise. If both noise are taken into account, this parameter is more effective for pulsewidth and TBP as shown in Table 4.4 and at this case, transform limited pulses are not generated because TBP is out of the range 0.3-0.5.

4.4.3   Spontaneous Coupling Factor

The spontaneous emission coupling factor (β factor) of a given mode is defined as the ratio of the spontaneous emission rate into that mode and the spontaneous emission rate into all modes. Spontaneous emission events happen to supply into the lasing field a fraction of spontaneous coupling factor (β_{sp}). This term is important for the dynamic behavior, without this term with P=0 at t=0 P would remin 0 [8, 34-36].
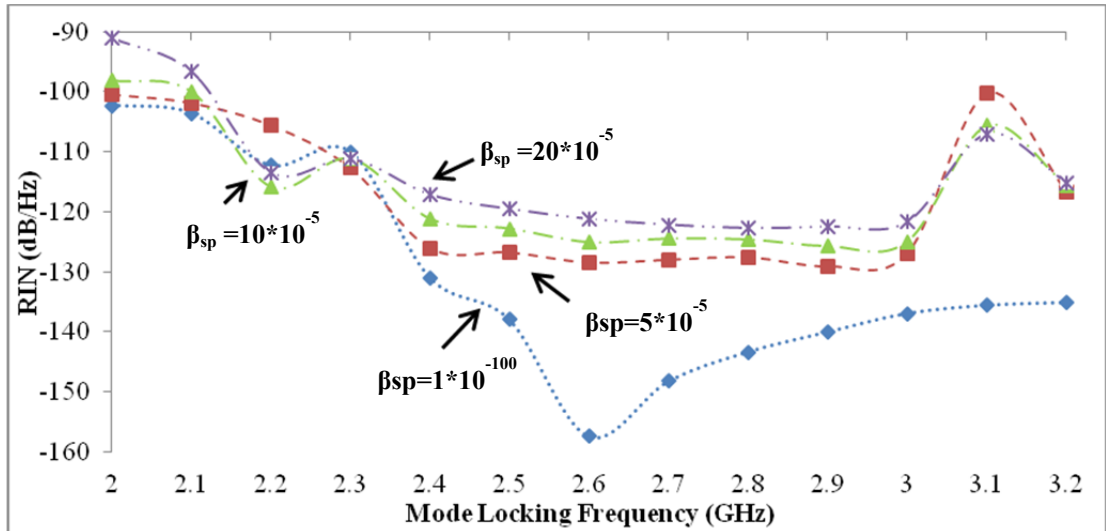
Figure 4.12 RIN Spectrums of HSPS with Sinusoidally Chirped Gaussian Apodized FBG for different β_{sp} with Spontaneous Noise.
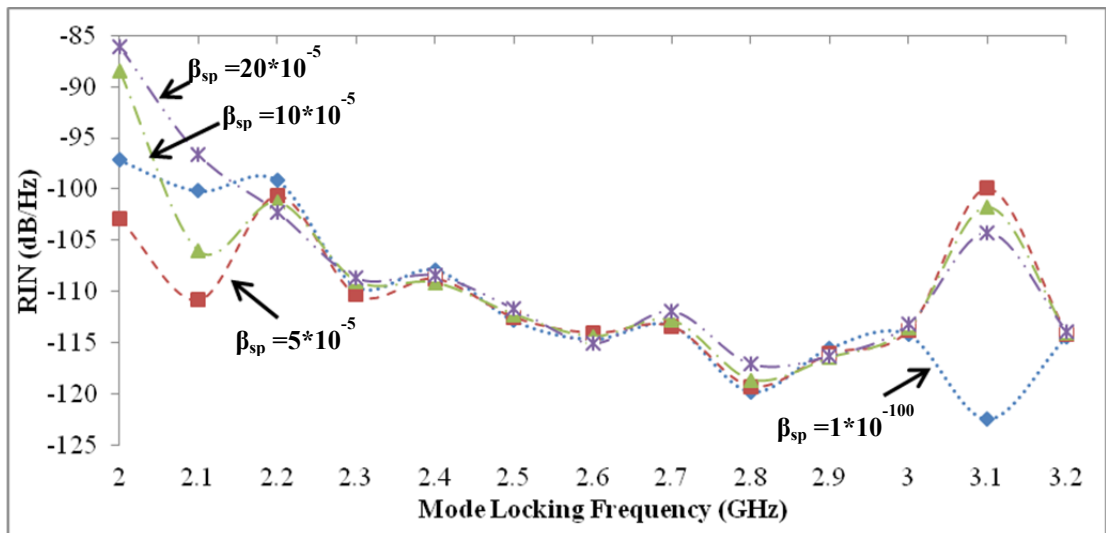
Figure 4.13 RIN Spectrums of HSPS with Sinusoidally Chirped Gaussian Apodized FBG for different β_{sp} with both Spontaneous and Carrier Noise.

Figure 4.12 and 4.13 show RIN spectrum of HSPS for sinusoidally chirped Gaussian-apodized FBG with spontaneous noise and both spontaneous and carrier noise and RIN increases with increasing β_{sp}, similarly linearly chirped Gussian-apodized FBG which was reported by Dogru *et al* [8, 51-52].

RIN spectrum is given in Fig. 4.12 if only spontaneous noise is considered. As seen in figure, for the standard parameter ($\beta_{sp}=5*10^{-5}$), transform limited pulses are generated at the mode-locking frequencies of 2.6 – 3 GHz. In this case, for the

fundamental mode-locking frequency of 2.5 GHz, RIN is -126.811 dB/Hz and for the other values of β_{sp}, RIN increases, except a value of $1*10^{-100}$. In this case, the value of RIN is -137.474 dB/Hz. Although TBP is in the range of the 0.3 and 0.5 at the mode-locking frequencies of 2.1, 2.3-2.5 and 3.2 GHz, transform limited pulses are not generated because the number of the peak in the frequency and field spectra are not equal to one. Therefore, these pulses are called as virtual pulses. Note that in the following figure, for the mode-locking fequencies 2 and 2.1 GHz, TBP values such as 0.523, 0.555 are not rounded to 0.5, therefore such pulses are not considered transform limited.

If both spontaneous and carrier noises are considered, RIN spectrum is shown in Fig. 4.13. Transform limited pulses are again generated at the same mode-locking frequencies for the standard value of β_{sp} as shown in Fig. 4.12, but the value of RIN is changed from -126.811 dB/Hz to -112.544 dB/Hz at the fundamental mode-locking frequency of 2.5 GHz, these results show the affect of the carrier noise on RIN spectrum.

As seen in the Table 4.5, pulsewidth, spectralwidth and TBP is slightly sensitive to β_{sp} with and without noise at the fundamental mode-locking frequency of 2.5 GHz for sinusoidlly chirped Gaussian-apodized FBG.

As seen in the Table 4.6, pulsewidth and TBP is sligtly sensitive to β_{sp} without noise, but this parameter is effective at the fundamental mode-locking frequency of 2.5 GHz with noise, in this case, as shown in Table 4.6, the values of TBP is 0.282 and 0.008 when spontaneous and both spontaneous and carrier noise are taken into account, respectively. The effect of this parameter on the spectralwidth is low with and without noise.

If both sinusoidally and linearly chirped Gaussian-apodized FBGs are compared, for producing short pulses with and without noise, sinusoidally chirped is more suitable than linearly chirped as shown in the Table 4.5 and 4.6.

Table 4 5 Effects of varying β_{sp} for sinusoidally chirped Gaussian-apodized FBG

β_{sp}	Pulsewidth (ps)	Spectralwidth (GHz)	TBP
10^{-100}	39.871*/39.363**/41.418***	9.287*/9.565**/9.847***	0.370*/0.376**/0.398***
$5*10^{-5}$	39.343*/39.068**/41.357***	9.299*/9.588**/9.805***	0.366*/0.375**/0.406***
$10*10^{-5}$	39.034*/38.813**/41.601***	9.274*/9.591**/9.768***	0.362*/0.372**/0.406***
$20*10^{-5}$	39.103*/38.716**/41.284***	9.232*/9.579**/9.747***	0.361*/0.371**/0.402***

Table 4 6 Effects of varying β_{sp} for linearly chirped Gaussian-apodized FBG

β_{sp}	Pulsewidth (ps)	Spectralwidth (GHz)	TBP
10^{-100}	45.405*/13.719**/31.473***	8.645*/8.948**/8.758***	0.393*/0.398**/0.036***
$5*10^{-5}$	45.381*/40.554**/1.278***	8.679*/8.604**/8.803***	0.394*/0.349**/0.011***
$10*10^{-5}$	45.467*/32.534**/0963***	8.714*/8.680**/8.814***	0.396*/0.282**/0.008***
$20*10^{-5}$	45.599*/3.989**/0.775***	8.729*/8.987**/8.686***	0.398*/0.036**/0.007***

*without noise   **with spontaneous noise   ***with both spontaneous and carrier noise

4.4.4   Field Coupling Factor

The effect of the field coupling factor (η) on the RIN spectrum is given in Fig. 4.14 and TBP of the output pulses are indicated in Fig. 4.15.

As seen in the Fig. 4.14, the RIN has a peak at 2.6 GHz for η=1, at 3 GHz for η=0.6 and at 3.1 GHz for η=0.8 and in this case, the value of RIN are -101.55 dB/Hz, -101.476 dB/Hz and -99.895 dB/Hz, respectively. At the corresponding frequencies, the value of TBP, 0.011, 0.012 and 0.012 are obtained as seen in the Fig. 4.15. Transform limited pulse is generated at the fundmental mode-locking frequency of 2.5 GHz when the value of η is 0.6. For the other field coupling factor, at the

fundamental mode-locking frequency of 2.5 GHz, transform limited pulses are not generated although TBPs are in the range of transform limited pulse specification (0.3-0.5), but the number of the peak in the frequency and field spectra are not equal to one. For the standard parameter (η=0.8), transform limited pulses are generated at the mode-locking frequency of 2.6-3 GHz. It is also observed that the range of the transform limited pulses are decreased with increasing of field coupling factor (η) with and without noise.
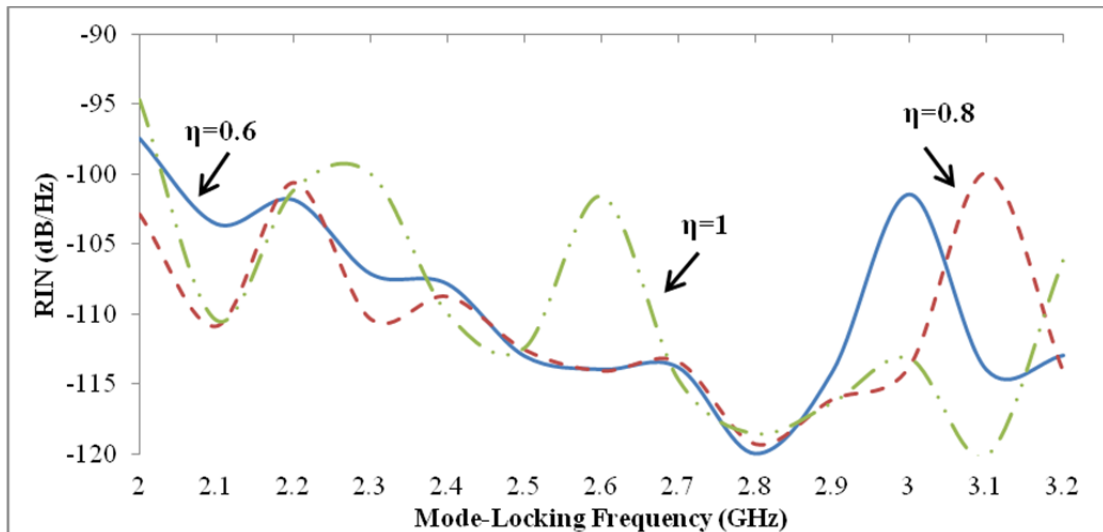
Figure 4.14 RIN Spectrums of HSPS with Sinusoidally Chirped Gaussian Apodized FBG for different values of field coupling factor (η) with both Spontaneous and Carrier Noise.
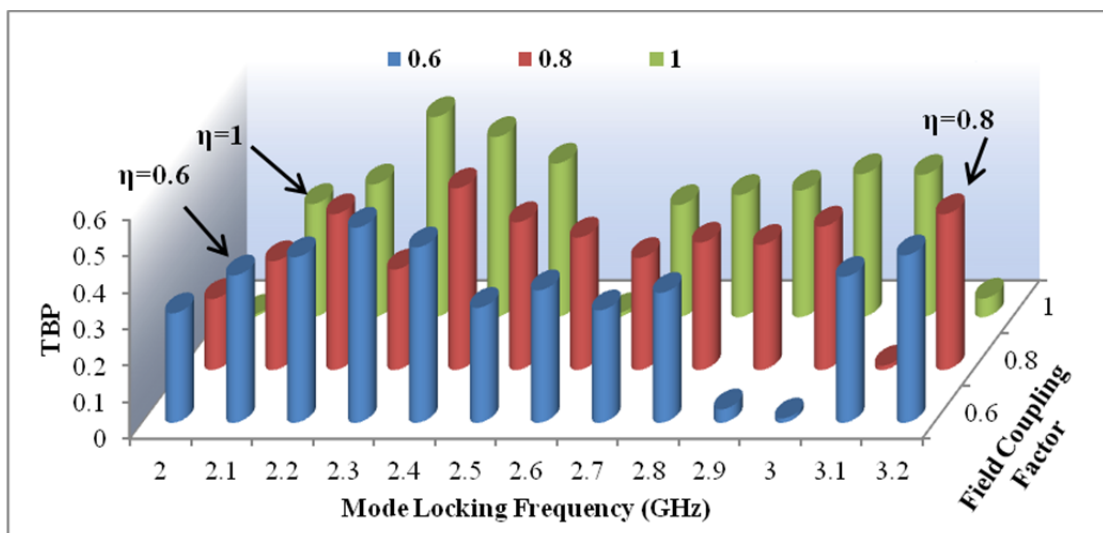
Figure 4.15 TBP of output pulses with Sinusoidally Chirped Gaussian Apodized FBG for different values of field coupling factor (η) with both Spontaneous and Carrier Noise.

4.5 Effects of Anti-Reflection Coefficient on TBP and RIN of HSPS

RIN spectrum of HSPS and TBP of output pulses with sinusoidally chirped Gaussian apodized FBG for different values of anti-reflection coefficient (AR) are shown in Figs. 4.16 and 4.17. The output pulses are also affected from this parameter with noise and without noise. AR coating is important for maximum field transfer to the fiber. In this study, it is taken 0.01 as a standard parameter. If anti-reflection coefficient (AR) is reduced from 0.01 to 0.001 then the peak power increases and the RIN also increases.

As seen in the Fig. 4.16, it has a peak where RIN is equal to -96,91 dB / Hz, at the fundamental frequency of 2.5 GHz and TBP is 0.009 as seen in Fig. 4.17. The transform-limited pulses are not generated for all mode-locking frequencies except for 3 GHz. Transform-limited pulses are generated between 2.8 and 3.1 GHz (300 MHz) and at 2.6 GHz for an AR value of 0.1. At the standard parameter (AR=0.01), the range which is transform limited pulses are generated between 2.6 and 3 GHz (400 MHz).

Figure 4.16 RIN Spectrums of HSPS with Sinusoidally Chirped Gaussian Apodized FBG for different values of anti-reflection coating reflectivity with both Spontaneous and Carrier Noise.

Figure 4.17 TBP of output pulses with Sinusoidally Chirped Gaussian Apodized FBG for different values of anti-reflection coating reflectivity with both Spontaneous and Carrier Noise.
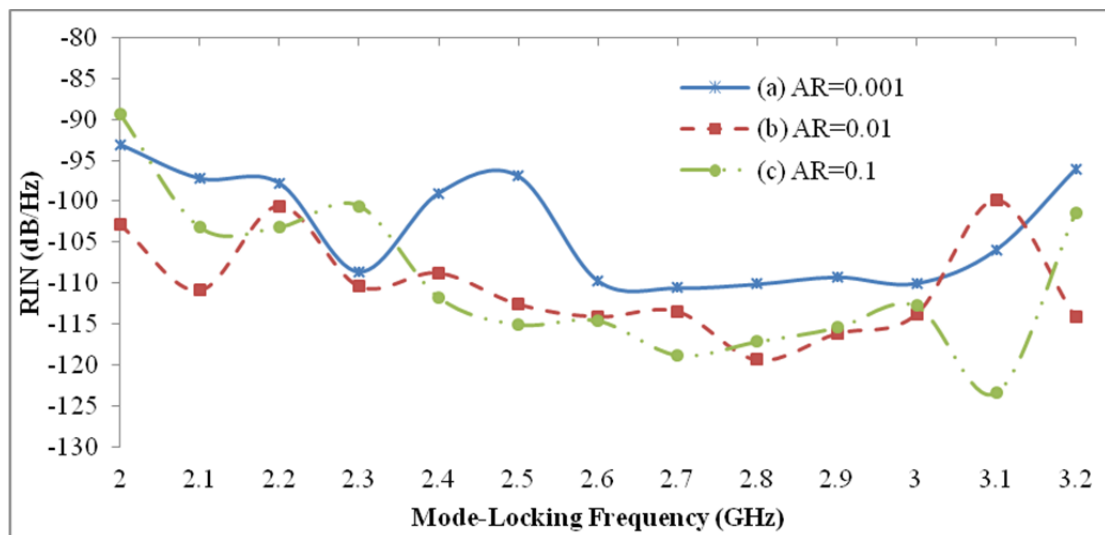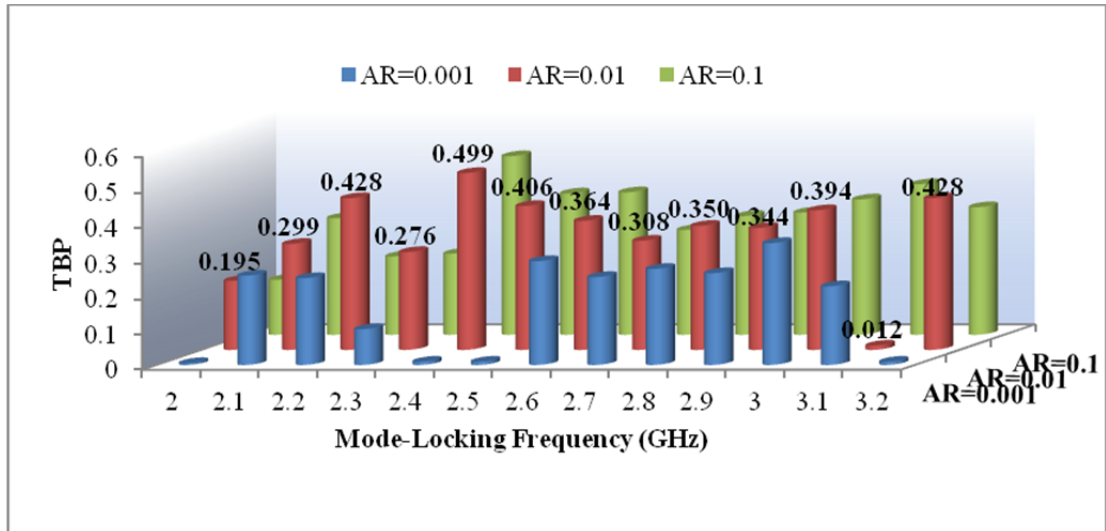
4.6   Effects of Reflectivity on TBP and RIN of HSPS

RIN spectrum of HSPS and TBP of output pulses with sinusoidally chirped Gaussian apodized FBG for different values of reflectivity are shown in Figs. 4.18 and 4.19. The output of the HSPS is taken at the end of the grating where $z=L/2$, according to this reason, the grating should not be a perfect reflector [54-58]. The reflectivity is selected to be relatively large in order to reduce to the cavity losses and keep the threshold current low. Therefore, the RIN spectrum is obtined for peak reflectivities of 0.3, 0.5, 0.7 and 0.99 as shown in Fig. 4.18 and 4.19. The TBP of the output pulses at the corresponding reflectivity is given in Fig. 4.19. As shown in the figures, the values of the RIN and TBP are nearly same for 0.3, 0.5 and 0.7 values of reflectivity. If reflectivity is taken to be 0.99, it means that approximately unity, discontunity occurs in group delay curve. The ideal reflection spectrum parameters for the mode-locked HSPS are which the reflection spectrum should have one lobe and group delay curve should be linear. If the value of the reflectivity increase then grating starts to get stronger, and the possibilty of the sidelobes occurence increases. If the results of Fig. 4.18 and 4.19 are examined, the generation of the transform limited pulses are shown easily. Transform limited pulses are generated between 2.5 and 2.9 GHz (400 MHz) and the RIN value of -114.789 dB/Hz for a peak

reflectivity of 0.3, between 2.6 and 3 GHz (400 MHz) and the RIN of -112.544 dB/Hz for a peak reflectivity of 0.5, and between 2.7 and 3.1 GHz (400 MHz) and the RIN of -112.139 dB/Hz for a peak reflectivity of 0.7 at the fundamental frequency of 2.5 GHz with both spontaneous and carrier noise. Also, as seen in the Fig. 4.18 and 4.19, transform limited pulses are generated between 2.2 - 2.6 GHz and 2.2 GHz when the values of the reflectivity is 0.99, respectively.

Figure 4.18 RIN Spectrums of HSPS with Sinusoidally Chirped Gaussian Apodized FBG for different values of reflectivity with both Spontaneous and Carrier Noise.
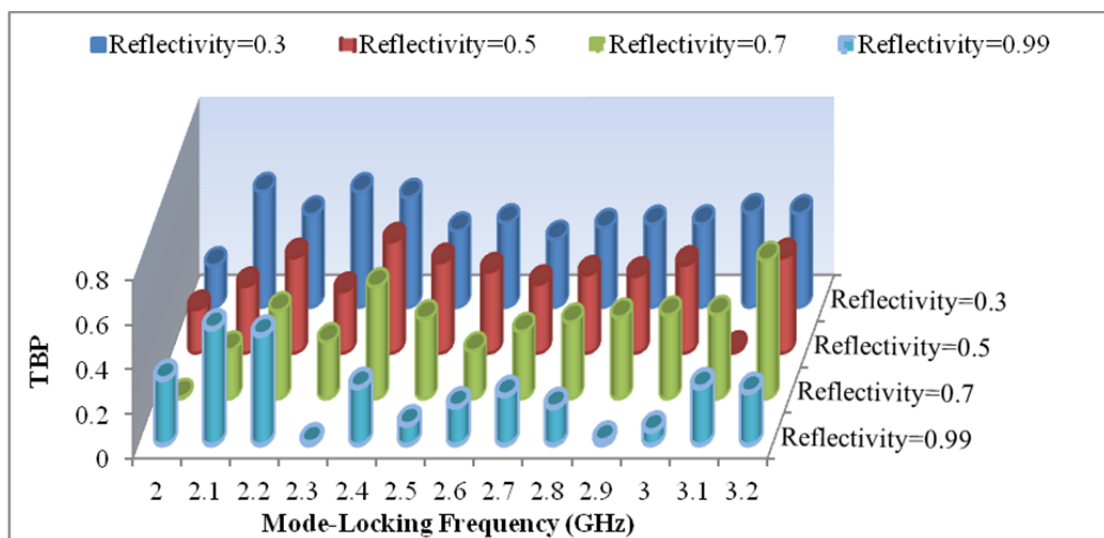
Figure 4.19 TBP of output pulses with Sinusoidally Chirped Gaussian Apodized FBG for different values of reflectivity with both Spontaneous and Carrier Noise.

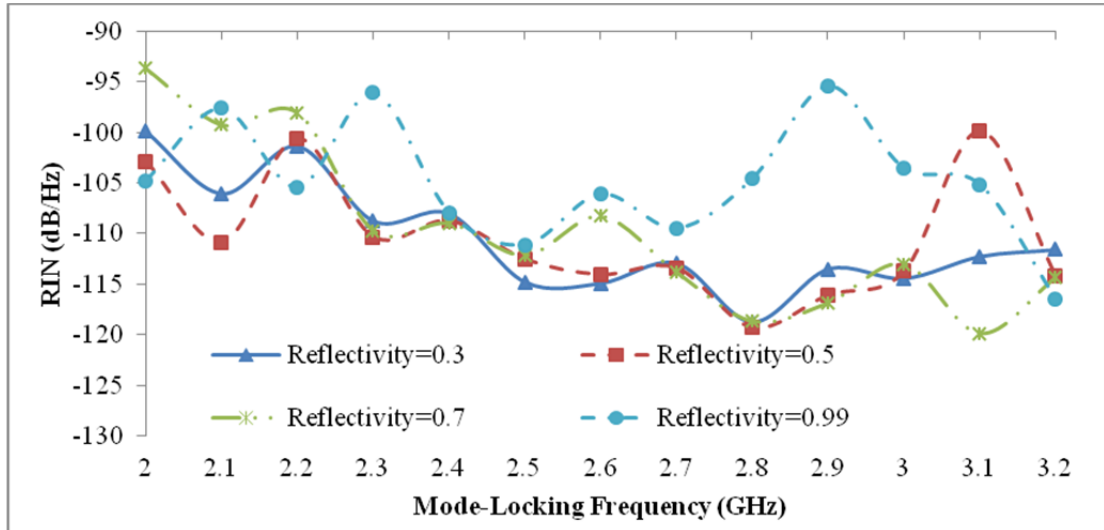## 4.7   Effects of External Cavity Length on RIN of HSPS and TBP

The effect of the external cavity length on the relative intensity noise (RIN) spectrum and time-bandwith product (TBP) is given in Figs. 4.20 and 4.21. As seen in the Fig. 4.20, RIN is inversely proportional to grating length. If the grating length decreases, the RIN increases or vice versa.
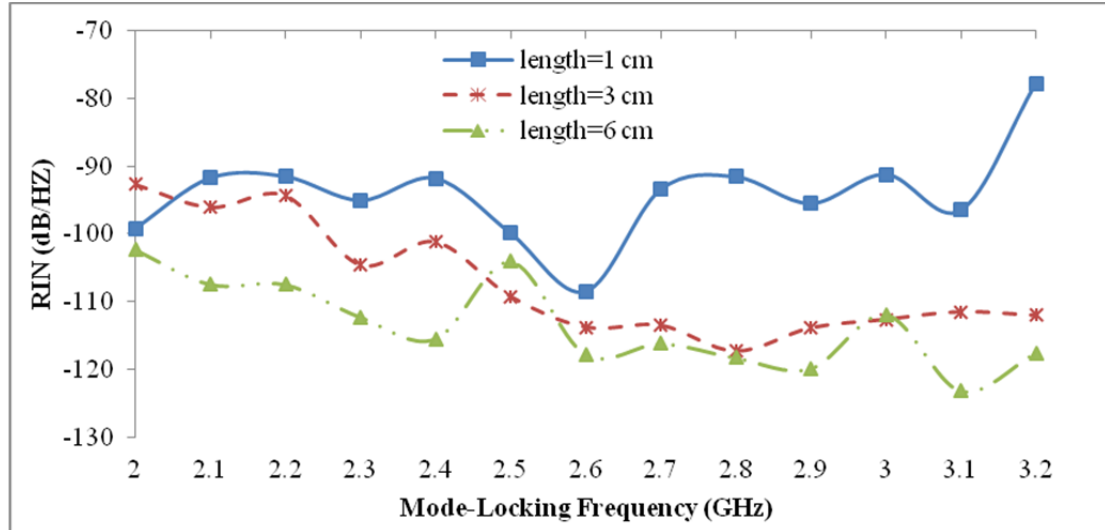
Figure 4.20 RIN Spectrums of HSPS with Sinusoidally Chirped Gaussian Apodized FBG for different values of external cavity length with both Spontaneous and Carrier Noise.
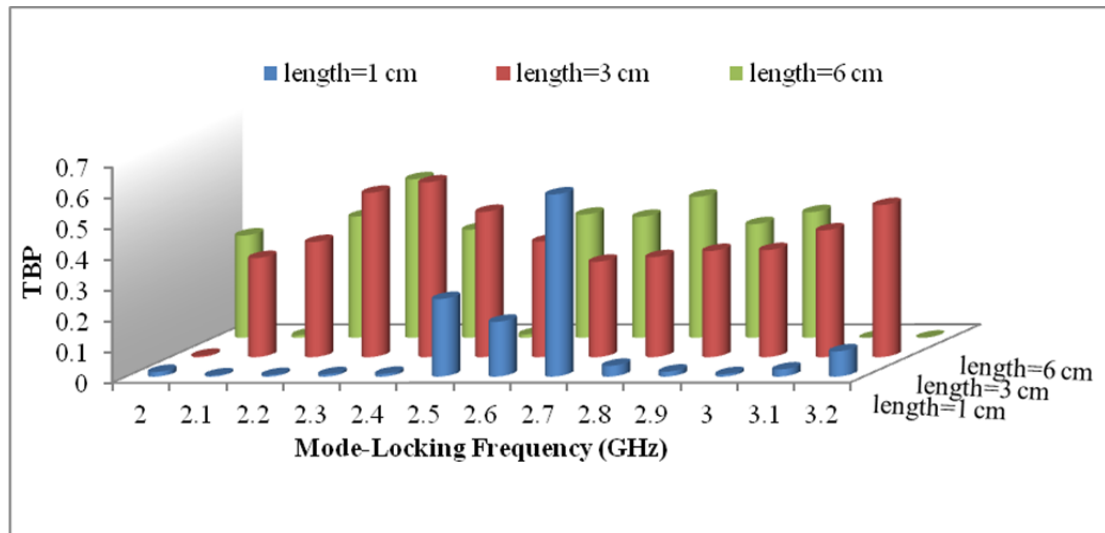
Figure 4.21 TBP of output pulses with Sinusoidally Chirped Gaussian Apodized FBG for different values of external cavity length with both Spontaneous and Carrier Noise.

If the pulse TBP is less than 0.3 or greater than 0.5, it means, that pulse is not transform-limited as seen in the Fig. 4.21 for all of the mode-locking frequencies. If

grating length is short then the shortest pulsewidths are produced and pulsewidths are also inversely proportional to the peak power.

4.8 RIN Reduction using Sinusoidally Chirped FBG in Mode-Locked HSPS

In this section, RIN reduction will be investigated in mode-locked HSPS when low and high spontaneous noise and both spontaneous and carrier noise are taken into account for linearly chirped and sinusoidally chirped Gaussian apodized FBGs. M. McAdams et al. [58] showed that at lower frequencies RIN reduction is possible by using an appropriate apodized grating with a continuous wave (CW) laser, and they demostrated 5 dB of RIN reduction. Using linearly chirped Gaussian apodized FBG, the relative intensity noise was also reduced 4 dB in a mode-locked HSPS by Dogru [8]. In the simulation, it is proved that the RIN reduction is possible at fundamental frequency of 2.5 GHz in a mode-locked HSPS utilizing sinusoidally chirped Gaussian-apodized FBG when we compared with linearly chirped Gaussian-apodized FBG.
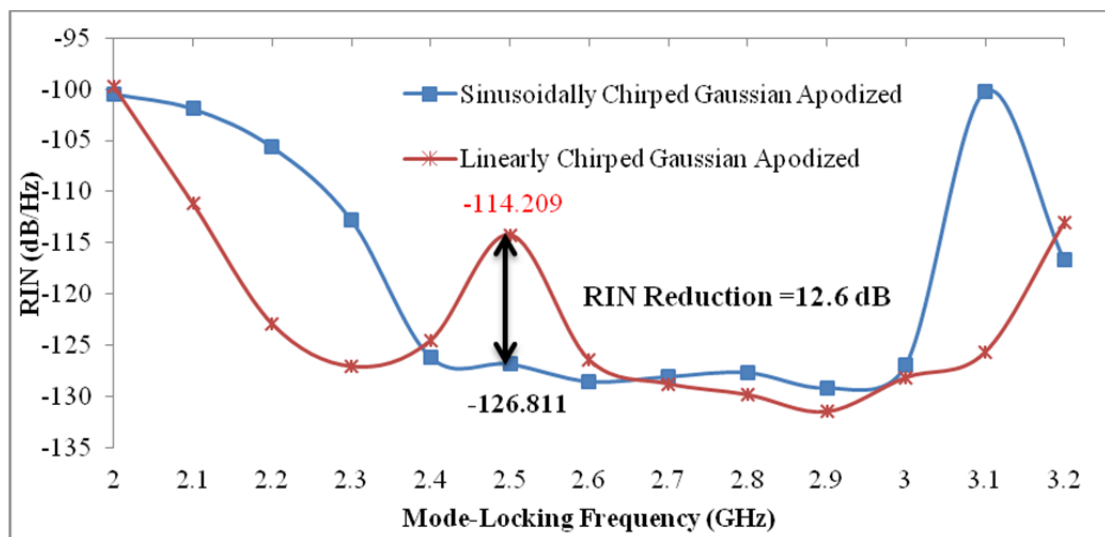
Figure 4.22 RIN Spectrums of HSPS with low Spontaneous Noise ($\beta_{sp}=5*10^{-5}$)

Figure 4.22 shows that 12.6 dB of RIN reduction is possible at the fundamental frequency of 2.5 GHz in a mode-locked HSPS utilizing a sinusoidally chirped Gaussian apodized FBG with low spontaneous noise, giving -126.811 dB/Hz peak value, where a value of -114.209 dB/Hz was obtained for corresponding linearly chirped Gaussian apodized FBG. At this time, pulsewidth, TBP and spectralwidth are

40.554 ps, 0.349 and 8.604 GHz for linearly chirped and 39.068 ps, 0.375 and 9.588 GHz for sinusoidally chirped Gaussian-apodized FBG, respectively.

Figure 4.23 shows the RIN versus mode-locking frequency of an HSPS with sinusoidally chirped and linearly chirped FBGs when low both spontaneous and carrier noise are taken into system. As seen in the figure 4.23, 9.64 dB of RIN reduction is possible at the fundamental frequency of 2.5 GHz. The peak value of RIN is -112.544 dB/Hz for sinusoidally chirped Gaussian-apodized FBG and -102.903 dB/Hz for linearly chirped Gaussian-apodized FBG, respectively. Pulsewidth, TBP and spectralwidth are 1.278 ps, 0.011 and 8.803 GHz for linearly chirped and 41.357 ps, 0.406 and 9.805 GHz for sinusoidally chirped Gaussian-apodized FBG.
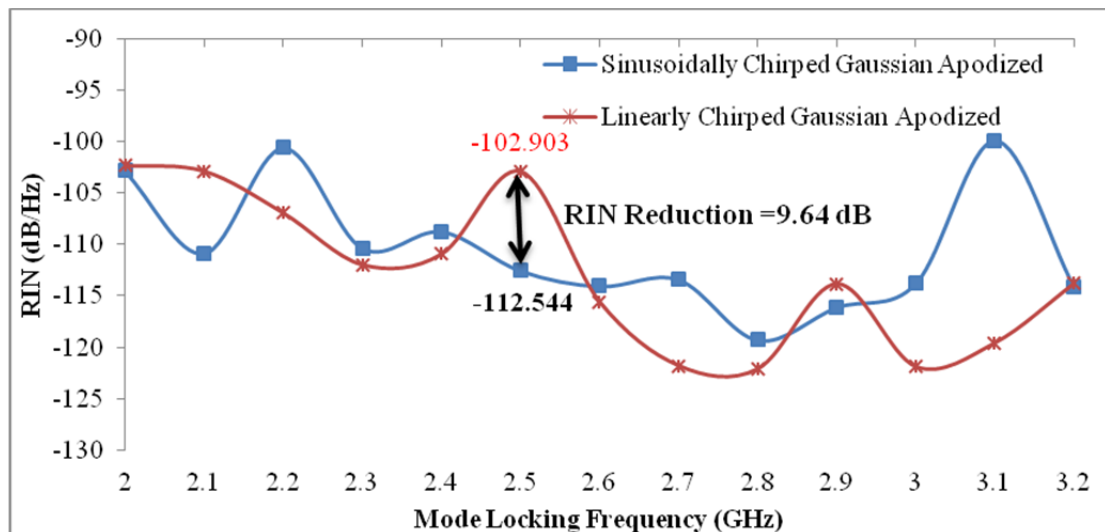
Figure 4.23 RIN Spectrums of HSPS with low Spontaneous and Carrier Noise ($\beta_{sp}=5*10^{-5}$)

According to Figure 4.24, it is found that 13.23 dB of RIN reduction is possible at mode-locking frequency of 2.5 GHz where high spontaneous noise is taken in the system and sinusoidally chirped Gaussian-apodized FBG is compared with linearly chirped Gaussian-apodized FBG. The peak value of RIN is -119.595 dB/Hz for sinusoidally chirped and -106.367 dB/Hz for linearly chirped Gaussian-apodized FBGs. Pulsewidth, TBP and spectralwidth are 38.716 ps, 0.371 and 9.579 GHz for sinusoidally chirped and 3.989 ps, 0.036 and 8.987 GHz for linearly chirped Gaussian-apodized FBGs.
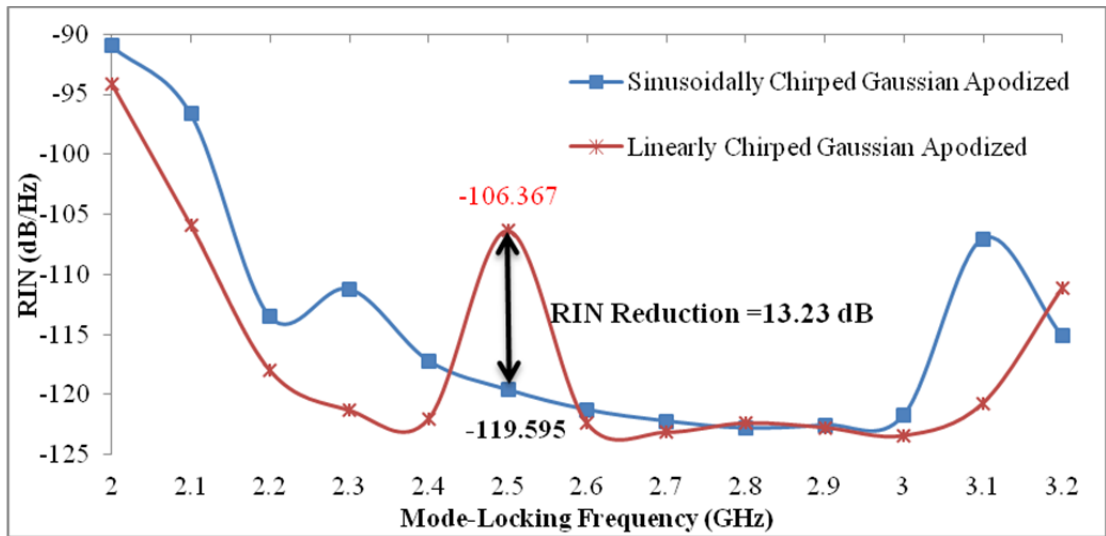
Figure 4.24 RIN Spectrums of HSPS with high Spontaneous Noise ($\beta_{sp}=20*10^{-5}$)
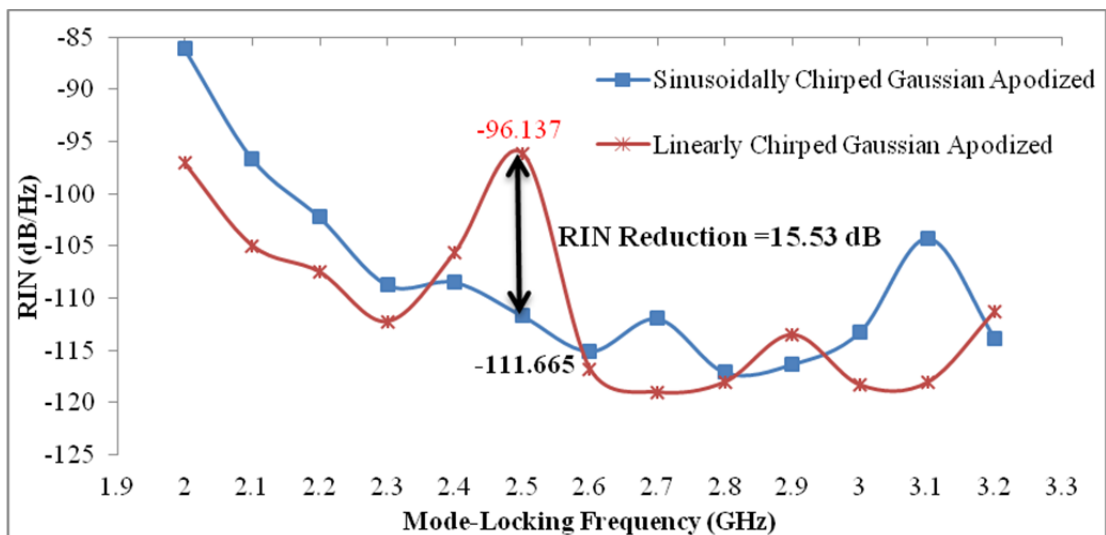
Figure 4.25 RIN Spectrums of HSPS with high Spontaneous and Carrier Noise ($\beta_{sp}=20*10^{-5}$)

If both high spontaneous and carrier noise are present in the HSPS system, a decrease in the RIN occurs as shown in Figure 4.25 when the results of sinusoidally chirped and linearly chirped Gaussian-apodized FBGs are compared each other. According to results where are shown in the Figure 4.25, it is found that 15.53 dB of RIN reduction using sinusoidally chirped Gaussian-apodized FBG. The peak values of RIN are -111.665 dB/Hz for sinusoidally chirped and -96.137 dB/Hz for linearly chirped Gaussian-apodized FBGs. Pulsewidth, TBP and spectralwidth are also

calculated 41.284 ps, 0.402 and 9.747 GHz for sinusoidally chirped and 0.775 ps, 0.007 and 8.686 GHz for linearly chirped Gaussian-apodized FBG.

CHAPTER 5

CONCLUSION

In this thesis, the relative intensity noise (RIN) and mode-locking characteristics of an HSPS utilizing a sinusoidally chirped Gaussian-apodized FBG were investigated by considering the effect of some laser diode and grating parameters. Our results showed that:

1. Even in the absence of noise, the effect of the grating and laser diode parameters are very strong on both the RIN spectrum and the output pulses of the HSPS.

2. Transform limited pulses are generated over a wider frequency range with sinusoidally chirped Gaussian-apodized FBGs with and without noise.

3. Noise increases with increasing value of linewidth enhancement factor, spontaneous coupling factor, and gain compression factor and with decreasing anti-reflection coefficient.

4. RIN value is also extremely sensitive to DC and RF current and noise increases with some value of these bias currents.

5. Transform limited pulses are generally obtained at the mode-locking frequencies between 2.6 – 3 GHz.

6. At the standard parameter, 9.64 dB of RIN reduction at the fundamental frequency of 2.5 GHz is possible in a mode-locked HSPS utilizing a sinusoidally chirped Gaussian-apodized FBG when compared with an HSPS with linearly chirped.

7. The range where transform limited pulses is generated decreases from 1.1 GHz (2.1-3GHz) to 400 MHz (2.6-3 GHz) when noise is taken into account.

However, HSPS is found to produce shorter pulses with sinusoidal chirped grating than with other types of gratings.

As a result, the capabilities of generating shorter pulses with and without noise and achieving 9.64 dB of RIN reduction at the fundamental mode locking frequency of 2.5 GHz make an HSPS utilizing a sinusoidally chirped FBG a candidate source for many applications such as OTDM, DWDM, and soliton propagation.

REFERENCES

[1] Hall R. N., Fenner G. E., Kingsley J. D., Soltys T. J., and Carlson R. O., (1962), "Coherent Light Emission From GaAs Junctions**",** *Phys. Rev. Lett.*, **vol. 9**, p. 366-368.

[2] Quist T. M., Rediker R. H., Keyes R. J., Krag W. E., B. Lax, McWhorter A. L., and Zeigler H. J., (1962), "Semiconductor Maser of GaAs", *Appl. Phys. Lett.*, **vol. 1**, p. 91.

[3] David F. Welch, Senior Member, (2000), "A brief history of high-power semiconductor lasers", *IEEE Journal of Selected Topics in Quantum Electronics* **vol. 6**, no. 6, pp. 1470-1477.

[4] Lang R. and Kobayashi K., (1980), "The relative intensity noise of a semiconductor laser subject to strong coherent optical feedback", *IEEE J. Quantum Electron.* **vol. 16,** p**.** 347.

[5] Cartaxo A. V. T. and Morgado J. A. P., (2000), "Analysis of semiconductor laser frequency noise taking into account multiple reflections in the external cavity*", IEE Proc. Optoelectron.,* **vol. 147**, p.335-344.

[6] P. W. Juodawlkis, J. C. Twichell, G. E. Betts, J. J. Hargreaves, R. D. Younger, J. L. Wasserman, F. J. O'Donnell, K. G. Ray, and R. C. Williamson, (2001), "Optically sampled analog-to-digital converters," Invited for Submission for the Special Issue on Microwave and Millimeterwave Photonics in a Joint Issue of the *IEEE Trans. Microwave Theory Tech. and the J. Lightwave Technol.*

[7] Leaf A. Jiang, Matthew E. Grein, *Student Member, IEEE,* Hermann A. Haus, *life Fellow, IEEE,* and Erich P. Ippen, (2001), "Noise of mode-locked semiconductor laser", *IEEE J. Quantum Electron.* **vol. 7,** no. 2**,** p**.** 159.

[8] Dogru, N., (2003), *"Effect of Noise on Mode-Locked Hybrid Soliton Pulse* of Gaziantep, Gaziantep.

[9] Petermann K., (1995), "External optical feedback phenomena in semiconductor lasers", *IEEE J. Sel. Top. Quantum Electron.* **vol. 1**, p. 480.

[10] Petersan P. M, *Biophotonics, 2nd International Graduate Summer School.*

[11] Schunk, N. And Petermann, K., (1998), "Numericl analysis of the feedback regimes for a single-mode semiconductor laser with external feedback.", *IEEE J. Quantum Electron.,* **vol. 24,** no. pp. 1242-1247.

[12] Kallimani K. I. and O' Mahony, M. J., (1998), " Relative intensity noise for laser diodes with arbitrary amounts of optical feedback.", *IEEE J. Quantum Electron.,* **vol. 4,** no. pp. 1438-1446.

[13] Rui J., Spencer P.S., and Shore K. A., (2004), "The relative intensity noise of a semiconductor laser subject to strong coherent optical feedback" *J.Opt B: Quantum Semiclass Opt,* **vol. 6**, p. 775-779.

[14] Wyatt, R. And Devlin, W. J. (1983). "10 kHz linewidth 1.5 μm InGaAsP external cavity laser with 55 nm tuning range.", *Electron. Lett.,* **vol. 19,** pp. 110-112.

[15] Kazanirov, R. F., Henry, C. H., and Olssan, N. A., (1987), " Narrow-band resonant optical reflectors and resonant optical trasformers for laser stabilization and wavelength division multiplexing.", *IEEE J. Quantum Electron.,* **vol. 23,** pp. 1419-1425.

[16] Olsson N. A., Henry, C. H., Kazanirov, R. F., Lee, H. J. And Orlowsky, K. J. (1988), "Performance characterisitcs of a 1.5 μm single frequency semiconductor laser with an external waveguide Bragg reflector." *IEEE J. Quantum Electron.,* **vol. 24,** no. pp. 143-147.

[17] Ferreira, M. F., Rocha, J. F. And Pinto, J. L., (1990), "Noise and modulation performance of Fabry-Perot and DFB semiconductor lasers with arbitrary external optical feedback.", *Proc. Ins. Elect. Eng.,* **vol. 137,** pp. 361-369.

[18] K. Gürs and R. Müller, (1963), "Breitband-modulation durch Steuerung der emission eines optischen masers (Auskopple-modulation)," *Phys. Lett.*, vol. 5, pp. 179–181.

[19] K. Gürs, (1964), "Beats and modulation in optical ruby lasers," in *Quantum Electronics III*, P. Grivet and N. Bloembergen, Eds. New York: Columbia Univ. Press, pp. 1113–1119.

[20] H. Statz and C. L. Tang, (1964), "Zeeman effect and nonlinear interactions between oscillating laser modes," in *Quantum Electronics III*, P. Grivet and N. Bloembergen, Eds. New York: Columbia Univ. Press, pp. 469–498.

[21] M. DiDomenico, (1964), "Small-signal analysis of internal (coupling type) modulation of lasers," *J. Appl. Phys.*, **vol. 35**, pp. 2870–2876.

[22] L. E. Hargrove, R. L. Fork, and M. A. Pollack, (1964), "Locking of He–Ne laser modes induced by synchronous intracavity modulation," *Appl. Phys. Lett.*, **vol. 5**, pp. 4–6.

[23] A. Yariv, (1965), "Internal modulation in multimode laser oscillators," *J. Appl. Phys.*, **vol. 36**, pp. 388–391.

[24] Bowers J.E. et al., (1989), "Actively mode-locked semiconductor lasers", *IEEE J. Quantum Electron.*, **vol. 25,** no.6. pp. 1426-1438.

[25] Morton, P. A., Mizrahi, V., Andrekson, P. A., Tanbun-Ek, T., Logan, R. A., Lemaire, P., Coblentz, D. L., Sergent, A. M., Wecht, K. W. and Sciortino Jr., P. F., (1993), "Mode-locked hybrid soliton pulse source with extremely wide operating frequency range.", *IEEE Photon. Tech. Lett.,* **vol. 5,** pp. 28-31.

[26] Olsson, N. A., Andrekson, P. A., Simpson, J. R., Tanbun-Ek, T., Logan, R. A. and Wecht, K. W. (1990). Opt. Fiber Commun. Conf. San Francisko, PD6.

[27] Ozyazici, M. S., Morton P. A., Zhang, L. M., Mizrahi V., (1995), "Theoretical model of hybrid soliton pulse source." *IEEE Photon. Tech. Lett.,* **vol. 7,** pp. 1142-1144.

[28] Sayın, M., (1999), "*Theoretical Model of the Mode-Locked Hybrid Soliton Pulse Source.",* Ph.D. Thesis, University of Gaziantep, Gaziantep.

[29] Pittoni. F., Gioannini M. And Montrosset, I., (2001), "Time-domin analysis of fiber bragg grating semiconductor laser operation in active mode-locking regime." *IEEE J. Select. Topics. Quantum Electron.,* **vol. 7,** no.2, pp. 280-286.

[30] Premaratne, M., Lowery. A. J., Ahmed, Z. And Novak, D., (1997), "Modeling noise and modulation performance of fiber grating external cavity lasers.", *IEEE J. Quantum Electron.,* **vol. 3,** no.2, pp. 290-303.

[31] Xia G., Wu Z. and Zhou H., (2003), "Influence of external cavity length on lasing wavelength variation of fiber grating semiconductor laser with ambient temperature", Optik, **vol. 114**, pp. 247-250.

[32] Quelltte F., (1987), "Dispersion cancellation using linearly chirped bragg grating filters in optical waveguides", *Opt. Lett.* **vol. 12,** pp. 847-849.

[33] Morton, P. A., Mizrahi, V., Andrekson, P. A., Tanbun-Ek, T., Logan, R. A., Lemaire, P., Coblentz, D. L., Sergent, A. M., Wecht, K. W. and Sciortino Jr., P. F. , (1993), "Mode-locked hybrid soliton pulse source with extremely wide operating frequency range." *IEEE Photon. Tech. Lett.,* **vol. 5,** pp. 28-31.

[34] Dogru N., (2012), "Sinusoidally chirped fiber Bragg grating for mode-locked application," *Journal of Optical Society of America B*, **vol. 29**, pp. 161-169.

[35] Ozyazici, M. S., Morton P. A., Zhang, L. M., Mizrahi V., (1995) , "Theoretical model of hybrid soliton pulse source.", *IEEE Photon. Tech. Lett.,* **7,** pp. 1142-1144.

[36] Dogru N. and Ersoy E., (July-August 2013), "RIN of mode-locked external cavity lasers utilizing a sinusoidally chirped fiber Bragg grating.", *IEEE J. Select. Topics. Quantum Electron.,* **vol. 18.**

[37] Hall R. N. et al., (1962), "Coherent light emission from GaAs junctions", Phys. Rev. Lett. 9 (9), 366.

[38] Holonyak N. and Bevacqua S. F., (1962), "Coherent (visible) light emission from Ga(AS1−xPx) junctions", Appl. Phys. Lett. 1, 82.

[39] Butler J. F. et al., (1965), "Properties of the PbSe diode laser", IEEE J. Quantum Electron. 1, 4.

[40] Wang C. A. and Groves S. H., (1992), "New materials for diode laser pumping of solid-state lasers", IEEE J. Quantum Electron. 28 (4), 942.

[41] Delfyett P. J. et al., (1992), "High-power ultrafast laser diodes", IEEE J. Quantum Electron. 28 (10), 2203.

[42] Endriz J. G. et al., (1992), "High power diode laser arrays", IEEE J. Quantum Electron. 28 (4), 952.

[43] Moloney J. V. et al., (2007), "Quantum design of semiconductor active materials: laser and amplifier applications", Laser & Photon. Rev. 1 (1), 24.

[44] Chow W. W. and Koch S. W., (1999), "Semiconductor-laser fundamentals", Springer, Berlin.

[45] Coldren L. A. and Corzine S. W., (1995), "Diode lasers and photonic integrated circuits", John Wiley & Sons, New York.

[46] Koechner W. K., (1999), "*Solid State Laser Engineering*," *Spriger-Verlag*, London.

[47] Kasap S. O., *Optoelectronics,* Prentice Hall.

[48] Guenther A., Pedrotti L. S. and Roychoudhuri C., (2003), "Lasers., *Fundamentals of Photonics.",* Module 5. pp. 1-44.

[49] Dogru N. and Ozyazici M. S., (2002), "Noise analysis for mode-locked lasers". General Assembly of URSI- International Union of Radio Science, Maastricht, Netherlands, 17-24 August, CD-ROM, Commission D, p.54-paper no.92.

[50] Dogru N. and Ozyazici M. S., (2004), "Effect of spontaneous and carrier noise on mode-locked hybrid soliton pulse source," *Opt. Quant. Electron.* **vol. 36**, pp. 527-537.

[51] Dogru N., (2009), "Effect of grating parameters on mode-locked external cavity lasers", *IEEE J. Sel. Top. Quantum Electron.* **vol. 15**, pp. 644-652.

[52] W. S. C Chang, (1969), "Solid state laser and gas laser amplifier and oscillator", *Quantum Electronics*. p. 200.

[53] McCumber, D. E., (1966), "Intensity fluctuations in output of cw laser oscillators," *Phys. Review*, **vol. 141**, pp. 306-322.

[54] C. H. Henry, (1982), "Theory of the linewidth of semiconductor lasers", IEEE J. Quantum Electron. **18** (2), p. 259.

[55] C. H. Henry, (1986), "Theory of spontaneous emission noise in open resonators and its application to lasers and optical amplifiers", *J. Lightwave Technol. LT-4*, p. 288.

[56] M. Osinski and J. Buus, (1987),"Linewidth broadening factor in semiconductor lasers – an overview", IEEE J. Quantum Electron. QE-23 (1), p. 9.

[57] McAdams M., Provenzano M., Peral D., Yariv .E, (2004), "Effect of transmission through-fiber gratings on semiconductor laser intensity noise", *App. Phys. Lett.,* **vol. 25,** pp.151-157.

[58] Chang W. S. C., (2005), "Principles of lasers and optics", *Cambridge University Press*, pp. 210-212.